Searches for electroweak production of supersymmetric particles with the ATLAS detector

PHENO 2020

Jason Oliver

~

jaoliver@cern.ch

This is me!

This is where I'm based

Adelaide, Australia

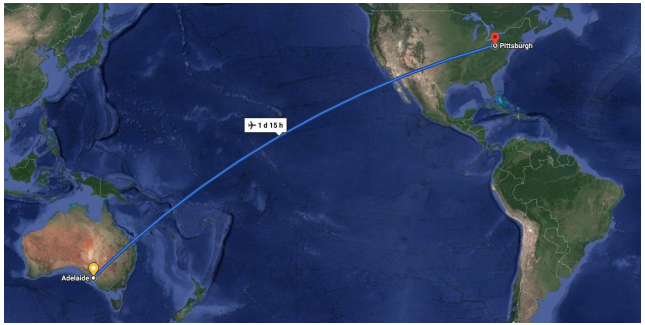

Introduction and Goals for today

- We have now collected enough data at the LHC to be sensitive to electroweak production of sparticles so its an exciting unexplored region to search for supersymmetry
- There are some open questions about supersymmetry
- My goal today is to explain two recent analyses which search for supersymmetry in different ways

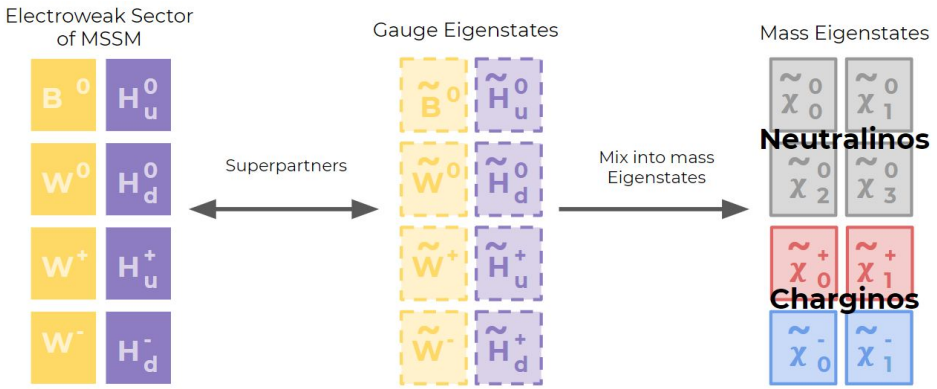

Open Questions

- How do the electroweak superpartners mix to form mass eigenstates, and what are their masses?
- Is the lightest one stable via R-Parity Conservation?
- If R-Parity is violated what is the nature of their decay?
- What signatures do they produce?

Search for trilepton resonances from chargino and neutralino pair production in $\sqrt{s}$ = 13 TeV pp collisions with the ATLAS detector

[ATLAS-CONF-2020-009]

Motivation

- A MSSM model which introduces a new U(1) symmetry and allows for R-Parity violation
- The sneutrino vev breaks $U(1)_{B-L}$ and R-Parity
  - RPV couplings are small due to the connection to the light neutrinos
- The LSP and chargino can decay to a lepton and a W/Z/H via a RPV coupling
- The search is performed in a resolution-corrected trilepton invariant mass mZl

Di-chargino production

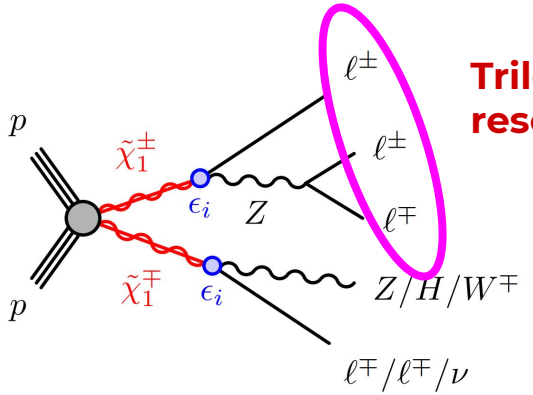

Trilepton resonance m_{Zl}

Chargino-neutralino production

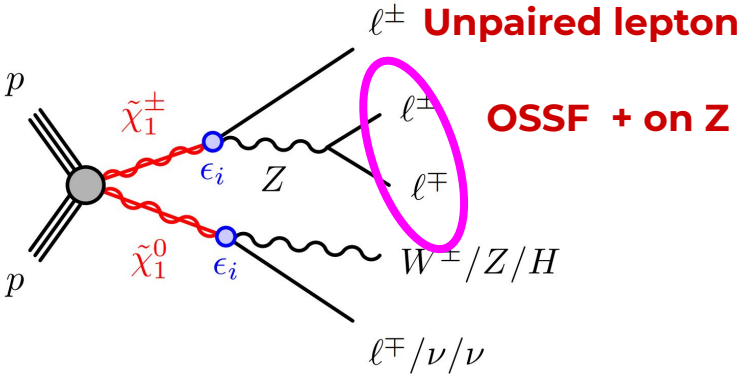

Unpaired lepton

OSSF + on Z

Event Categorisation into Signal Regions

We trigger on at least one electron or muon with Isolation and pt requirements
(see backup for details)

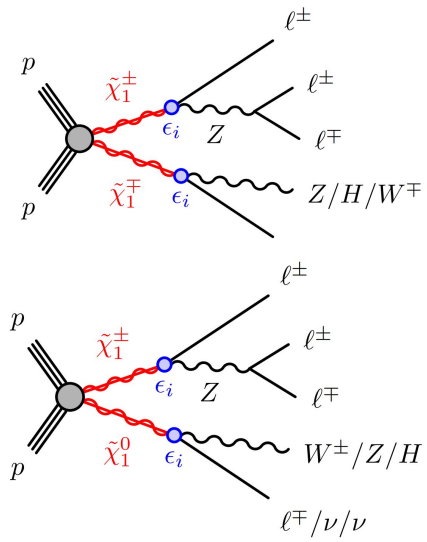

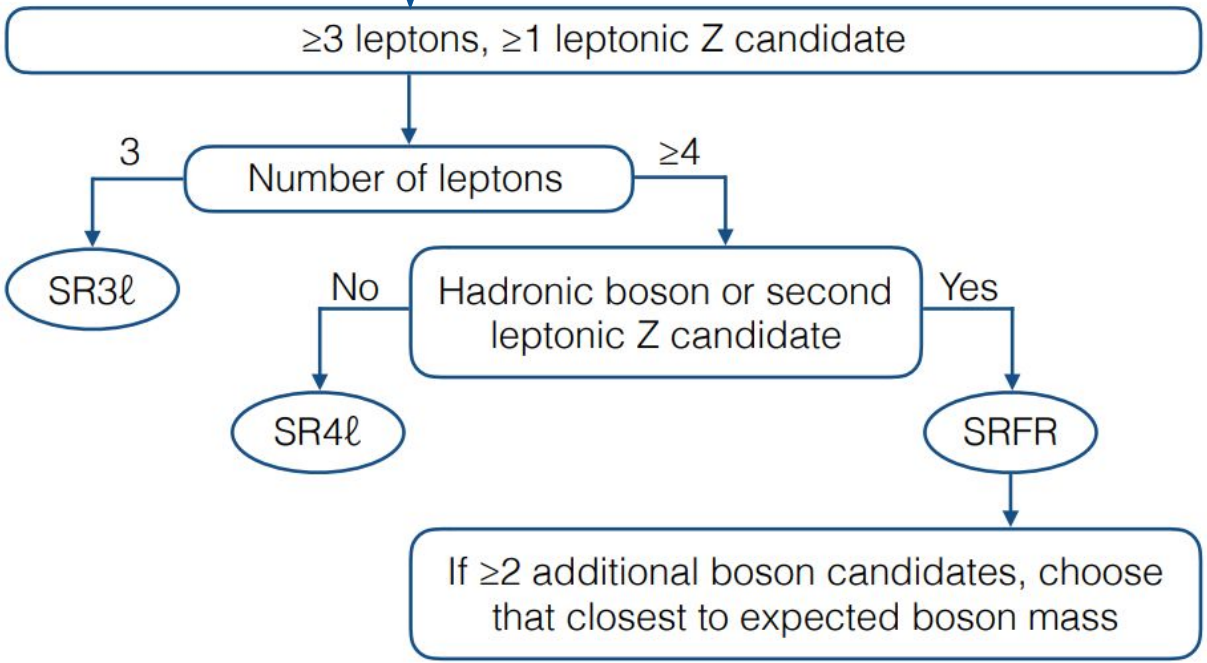

Our Three Scenarios

- For SRFR and SR4L the major backgrounds are ZZ and ttZ
- ZZ removal : for events with 4 leptons, can't have a 2nd mll pair with invariant mass within 20 GeV of the Z
- ttZ removal: for events with 2 btagged jets we require $\Delta R(b1,b2) < 1.5$ - consistent with a Higgs in the signal.
- Normalised to data using a control + validation region approach

ZZ background Removal

1st lepton pair

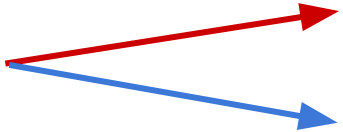

SFOS
mll ON-Z mass

2nd lepton pair

mll OFF-Z mass

ttZ background Removal

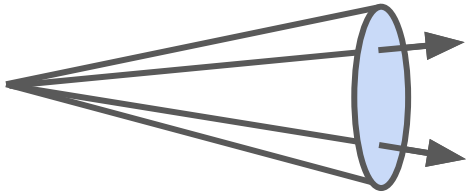

B-tagged jets need to be close

Our control region + validation region strategy

Variable: The 2nd lepton pair mll

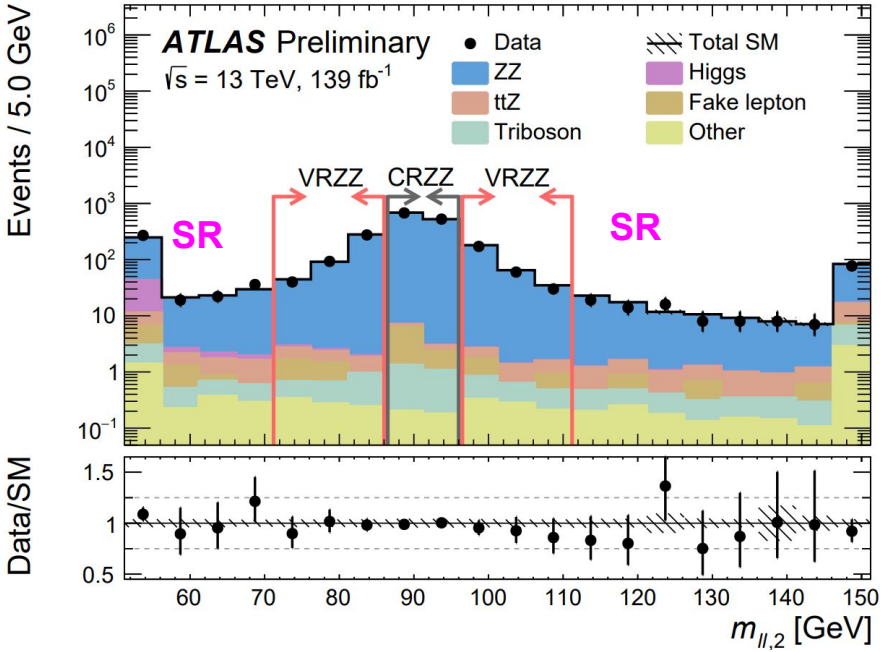

Variable: ΔR(b1,b2)

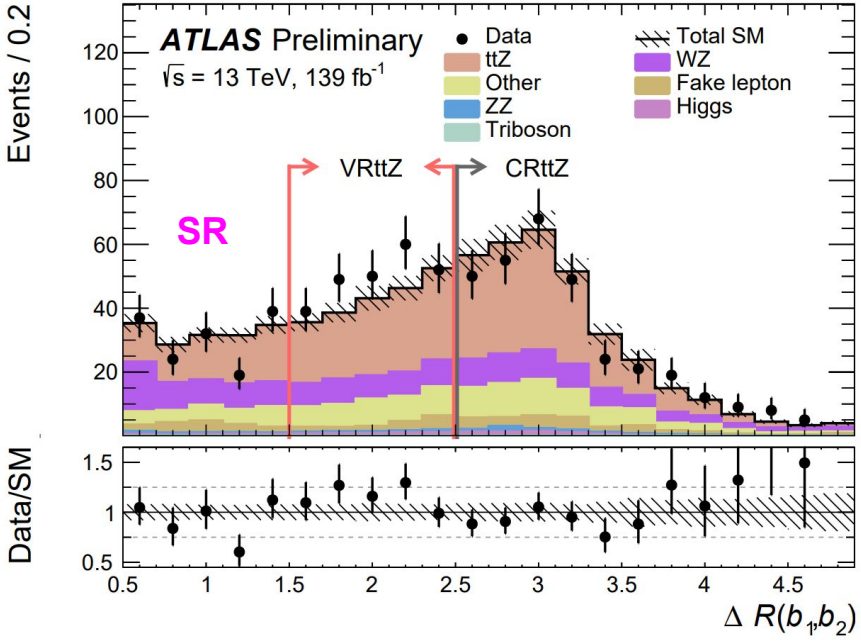

Data / SM Estimate is good in our CR and VRs

Signal Region Results

- mZl masses of 100 to 1500 GeV were explored by the search
- 3 benchmark signal points were chosen - 200GeV, 500GeV and 800GeV
- We see good agreement between Data and SM expectation
- We can interpret these results into model independent results (shown in backup) and cast them as model dependent exclusions
- All signal regions are shown in the backup

SRFR

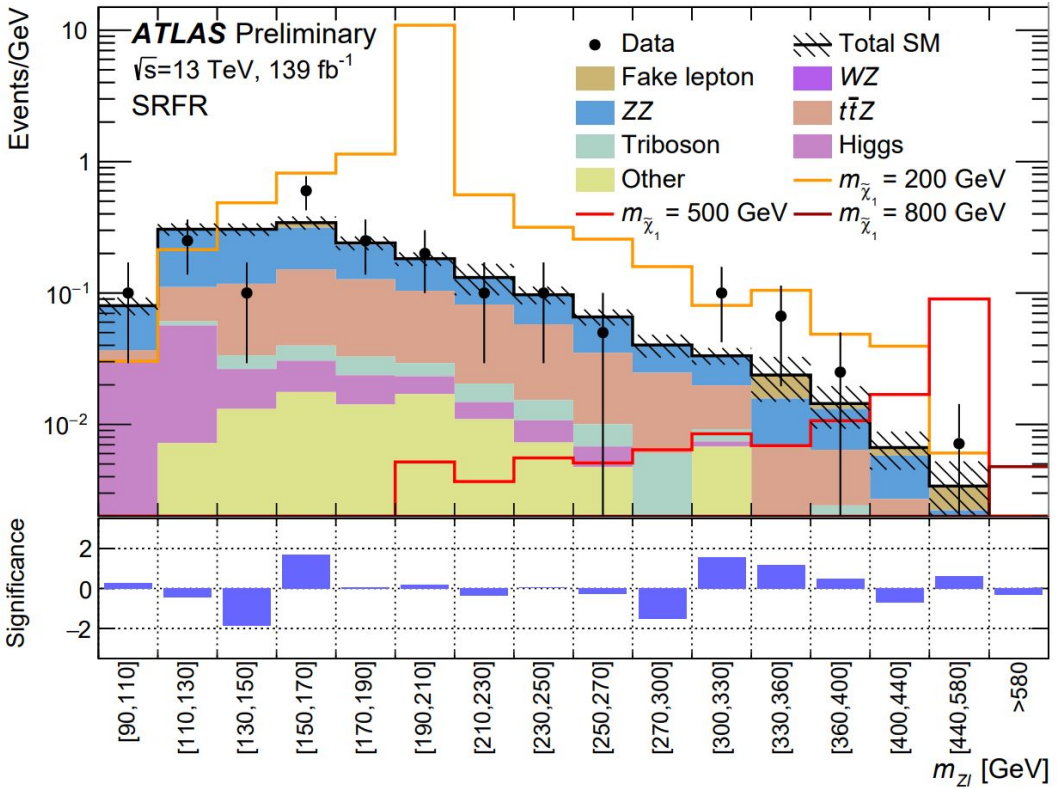

- Set model dependent exclusion limits on chargino/neutralino masses by scanning branching fractions to Z
- Exclusions are largest when branching fraction to Z is 100%
  - 1050 GeV for electrons
  - 1000 GeV for muons
  - 625 GeV for taus
  - 950 GeV for inclusive fit
- At 1% Branching Fraction to Z
  - 300 GeV for electrons
  - 375 GeV for muons
  - No limit for tau

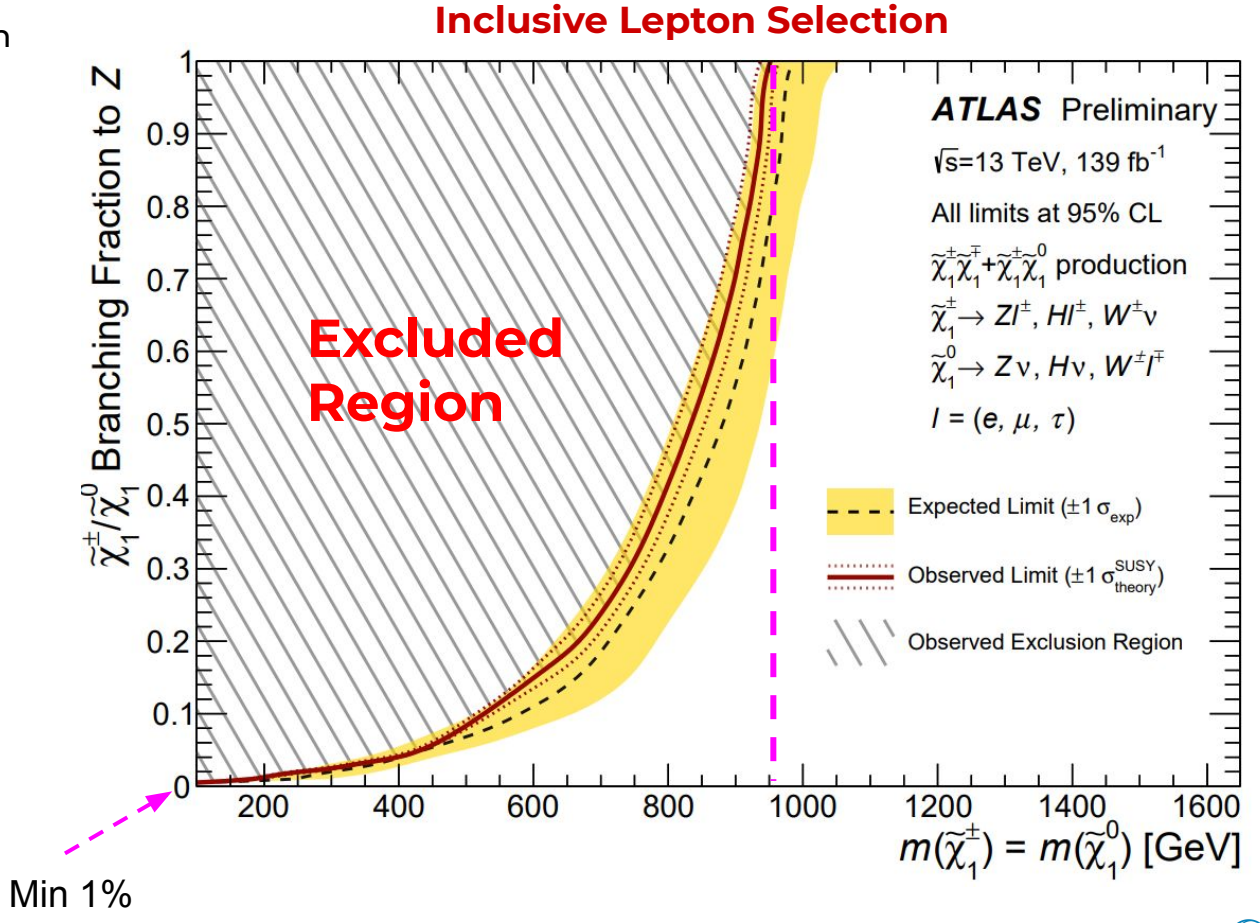

Searches for electroweak production of supersymmetric particles with compressed mass spectra in √s=13 TeV pp collisions with the ATLAS detector

LINK

Compressed Approach

- R-Parity is conserved, and the LSP is close in mass to a heavier SUSY partner such as a chargino or 2nd neutralino or slepton.
- Small mass splitting between particles leads to very soft decay products that are difficult to identify & reconstruct
- An initial state radiation kick can increase MET and and increases sensitivity to the processes

Higgsino / wino-bino

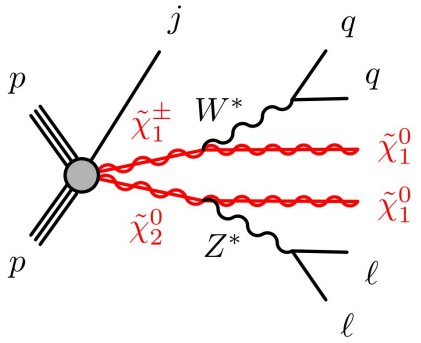

VBF t-channel

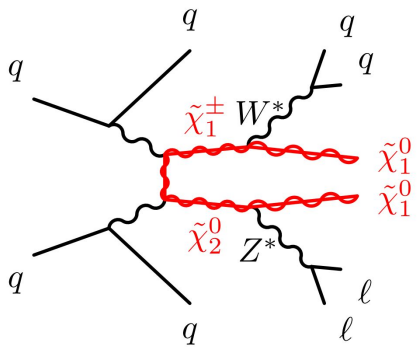

Slepton Scenario

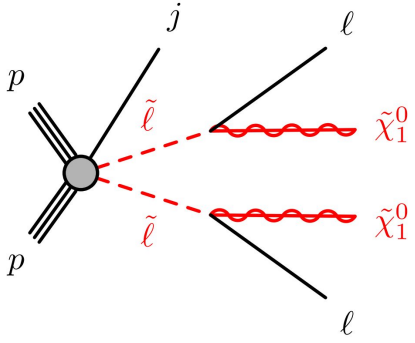

Signal Region approach

- 3 EWK SRs split by MET targeting ISR production
- 1 EWK SR targeting high MET with 1 lepton + 1 track (Targets SUSY signals with very small Δm + MET)

Additional Signal Regions (not explored today)

- 2 VBF SRs with high and low $\Delta\eta$ between two leading jets.
- 2 Slepton SRs targeting 150 GeV < MET < 200 GeV and MET > 200 GeV

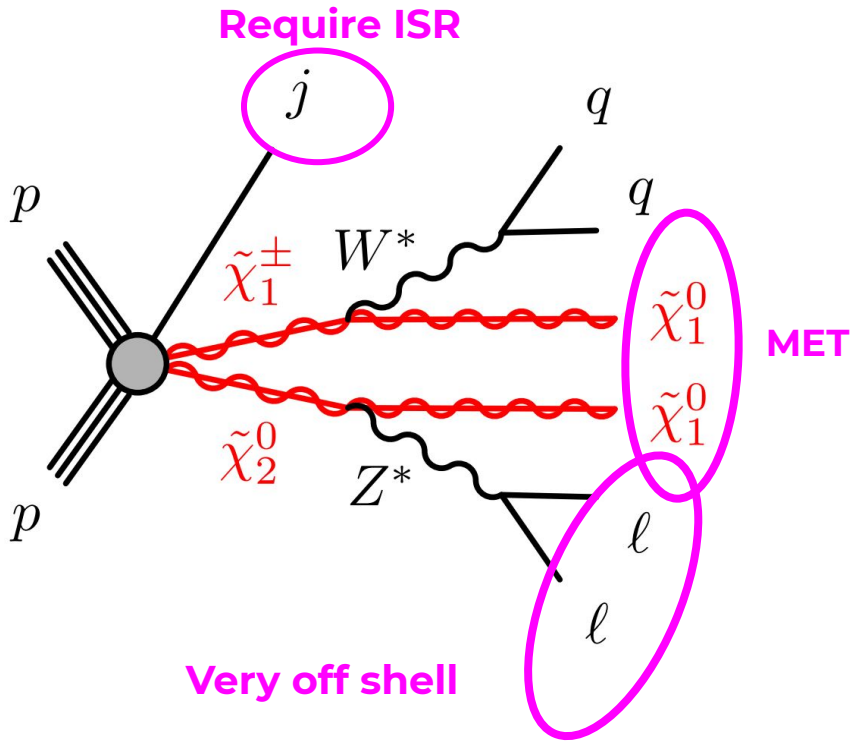

- Main background is 1 lepton + 1 track from hadron/ non prompt lepton
- Lepton pt < 10 GeV + track pt < 5 GeV
- **$\Delta\phi$(lep,pTMET) < 1.0** to reduce non-prompt backgrounds and **0.05 < ΔR(lep,track) <1.5**
- Signal track be within ΔR <0.01 of non-signal electron or muon candidate.
- The signal tracks must be ΔR > 0.5 of jets
- Signal track pT must be within 20% of the candidate pt
- Nearby preselected tracks must have a combined transverse momenta less than 0.5 GeV
- Signal track pT > 1GeV + impact parameter requirements

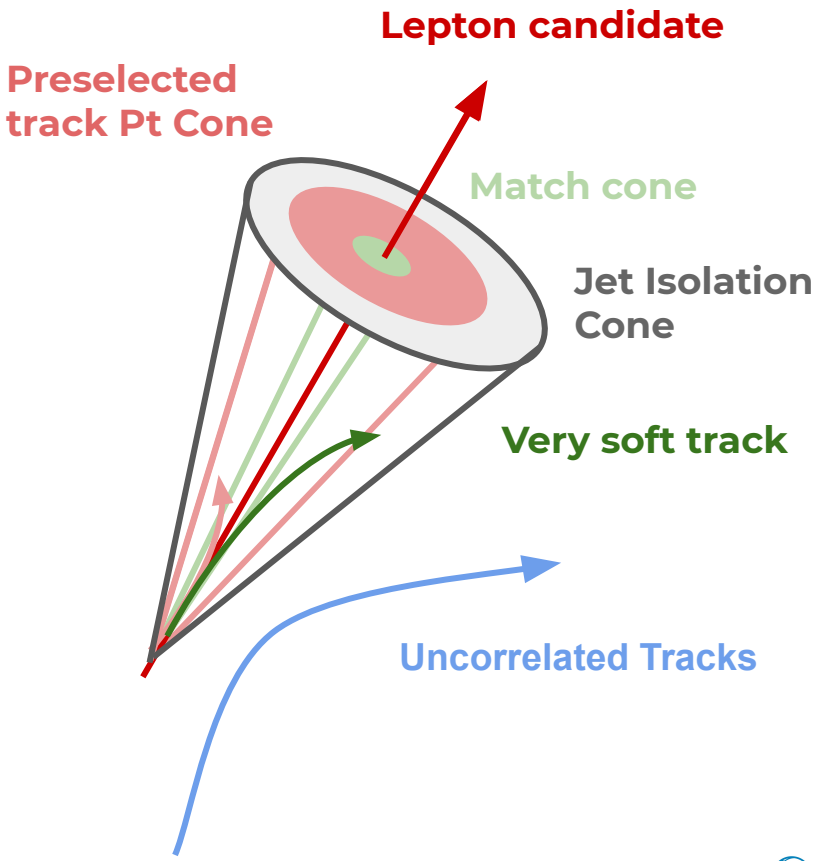

- Background of the 1 lepton 1 track Signal Region is estimated from SS selections
- Validate in two ways
  - W+jets MC
  - Data
- To test in data we define a VR
- Inverting the **$\Delta\phi$(lep,pTMET) > 1.0**
- Upper bound on **ΔR(lep,track)** is removed and other selections were loosened to increase statistics
- Confirmed the SS modelled OS in our region of interest

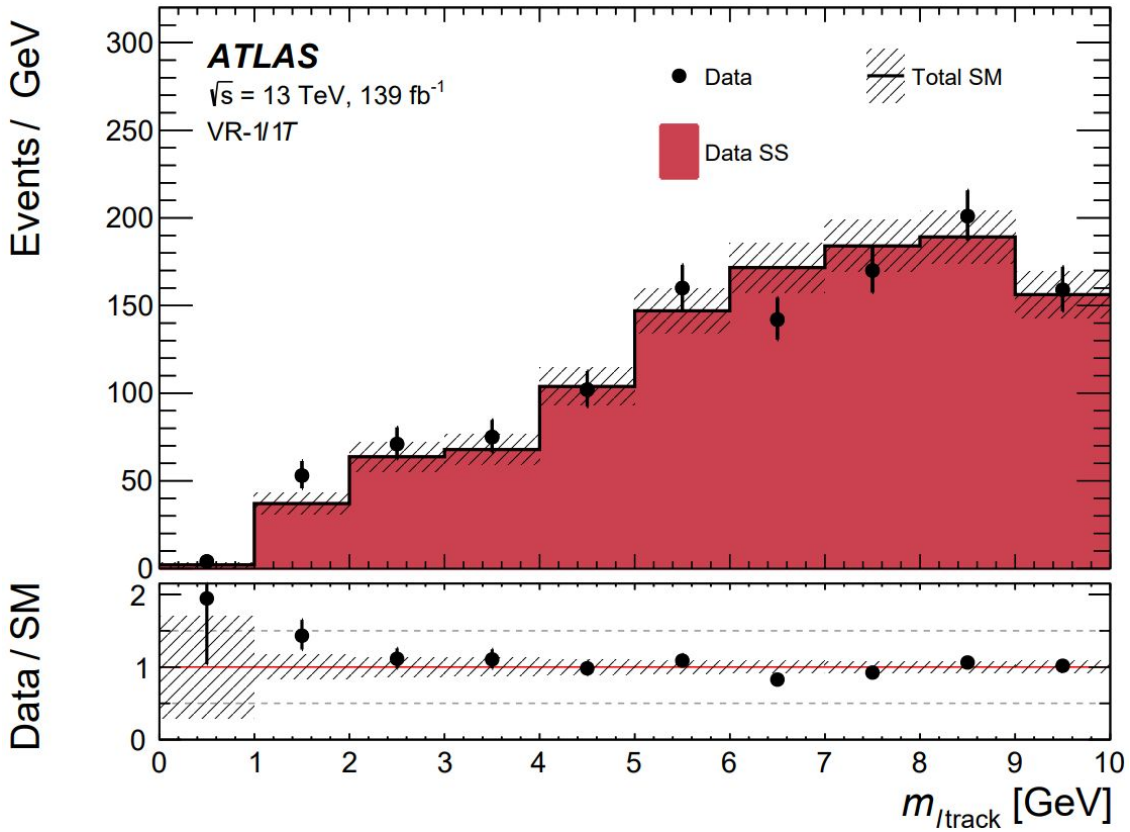

Post-fit Electroweak Signal Regions

- We see good agreement between data and estimates
- When we look at these regions inclusively we see no deviations above 2 sigma
- Two deficits in SRmumu-mll and SRee-mll
- In particular we see nice agreement with the 1 lepton + 1 track signal region

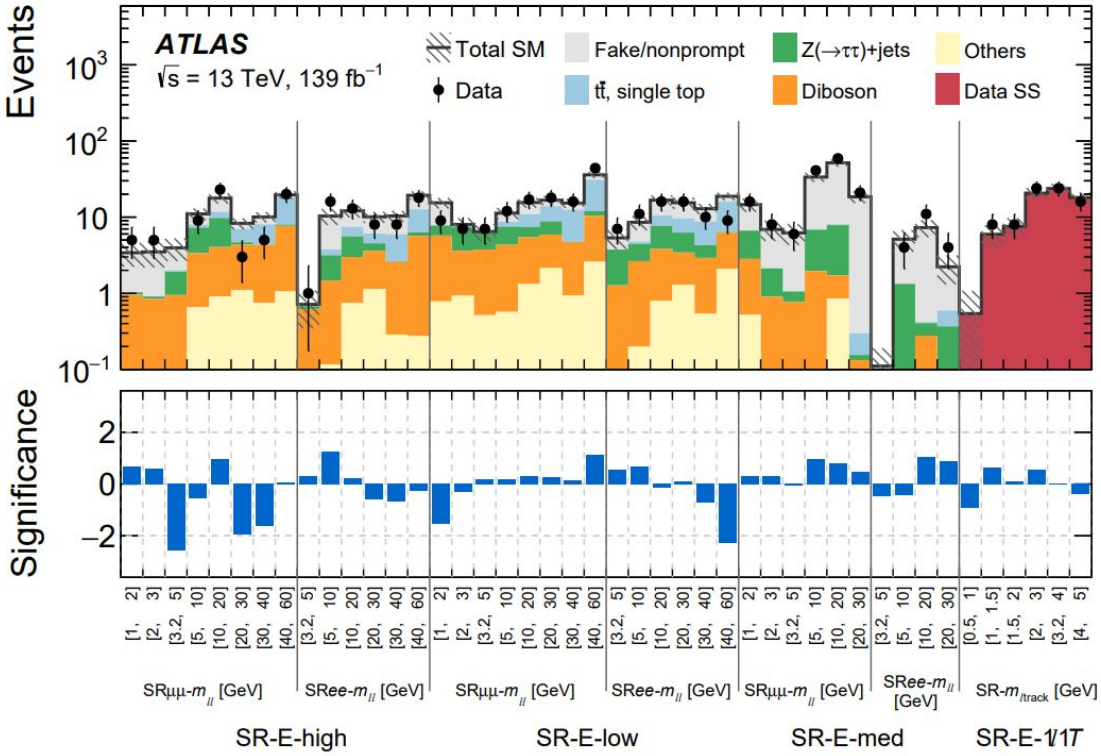

- Exclusions are in Δm(N2,N1) vs m(N2) space.
- They depend on the mixing of the neutralino / charginos
- Different mixing hypotheses produce different mll distributions and therefore different exclusions
- The inclusion of the 1lepton + 1 track signal region extended the exclusions in the very small mass differences region

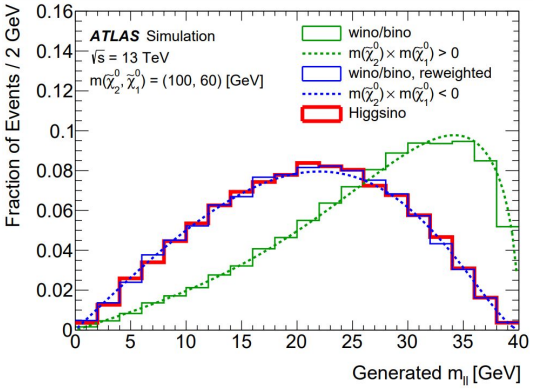

Higgsino Scenario

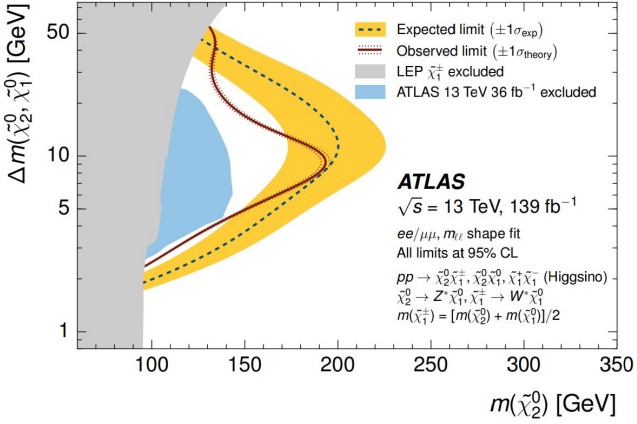

Wino/Bino Positive N2N1 mass product

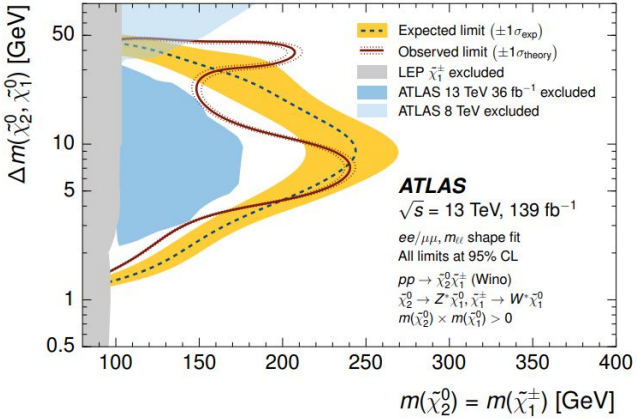

Wino/Bino Negative N2N1 mass product

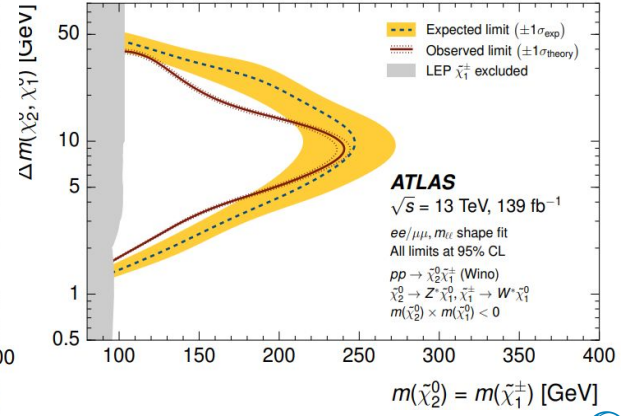

Concluding Remarks

- ATLAS has published a number of analyses targeting different SUSY scenarios
- The electroweak sector of SUSY remains an broad area with rich phenomenology
- The final state will continue to present many difficult challenges which demand new techniques and approaches
- Stay tuned!
- To find a complete list of all public SUSY searches in ATLAS
- https://twiki.cern.ch/twiki/bin/view/AtlasPublic/SupersymmetryPublicResults

Additional Material

3L B-L MSSM ADDITIONAL MATERIAL

Table 1: Details of the Monte Carlo simulation for each physics process, including the event generator used for matrix element calculation, the generator used for the PS and hadronization, the PS parameter tunes, and the order in α_S of the production cross section calculations.

Process	Event generator	PS and hadronization	PS tune	Cross section (in QCD)
Diboson, Triboson, (Z+jets)	Sherpa 2.2	Sherpa 2.2	Default	NLO (NNLO)
$t\bar{t}W$, $t\bar{t}Z$, (Other top)	MadGraph5_aMC@NLO 2	Pythia 8	A14	NLO (LO)
$t\bar{t}$, (tW), [$t\bar{t}H$]	Powheg-Box v2	Pythia 8	A14	NNLO+NNLL (NLO+NNLL) [NLO]
Higgs: ggF, (VBF, VH)	Powheg-Box v2	Pythia 8	AZNLO	NNNLO (NNLO+NNLL)
$\tilde{\chi}_1^{\pm}\tilde{\chi}_1^{\mp}$, $\tilde{\chi}_1^{\pm}\tilde{\chi}_1^{0}$	MadGraph 2.6	Pythia 8	A14	NLO+NLL

Table 2: Selection criteria for the various signal, control, and validation regions used in the analysis. All regions require a pair of leptons with the same flavor and opposite sign of their electric charge whose invariant mass is between 81.2 GeV and 101.2 GeV. They additionally require a third lepton and a trilepton invariant mass above 90 GeV. The 2nd boson requirement indicates the presence of two additional jets or leptons consistent with a W, Z, or Higgs boson decay. The asterisk (*) in the SR4ℓ $E_{\mathrm{T}}^{\mathrm{miss}}$ requirement indicates that this selection is only considered for events with two pairs of same-flavor leptons. The $\Delta R(b_1, b_2)$ selection is only considered for events with at least two b-jets.

Region	N_{lep}	$E_{\mathrm{T}}^{\mathrm{miss}}$ [GeV]	$m_{\mathrm{T}}^{\mathrm{min}}$ [GeV]	2nd boson	2nd leptonic Z; $\lvert m_{\ell\ell,2} - m_Z \rvert$ [GeV]	$N_{\mathrm{b-jet}}$	$\Delta R(b_1, b_2)$	$m_{Z\ell}^{\mathrm{asym}}$
SRFR	≥4	-	-	Yes	veto; <20	-	<1.5	< 0.1
SR4ℓ	≥4	>80*	-	No	veto; <20	-	<1.5	-
CRZZ	=4	-	-	-	require; <5	-	<1.5	-
VRZZ	=4	-	-	-	require; [5,20]	-	<1.5	-
CR$t\bar{t}Z$	≥3	>40	-	-	veto; <20	≥2	>2.5	-
VR$t\bar{t}Z$	≥3	>40	-	-	veto; <20	≥2	[1.5,2.5]	-
SR3ℓ	=3	>150	>125	-	-	-	<1.5	-
CRWZ	=3	<80	[50,100]	-	-	-	<1.5	-
VR$E_{\mathrm{T}}^{\mathrm{miss}}$	=3	>80	<100	-	-	-	<1.5	-
VR$m_{\mathrm{T}}^{\mathrm{min}}$	=3	<80	>125	-	-	-	<1.5	-
CRFake	=3	<30	<30	-	-	-	<1.5	-
VRFake	=3	[30,80]	<30	-	-	-	<1.5	-

Trilepton invariant mass modelling in each CR and VR

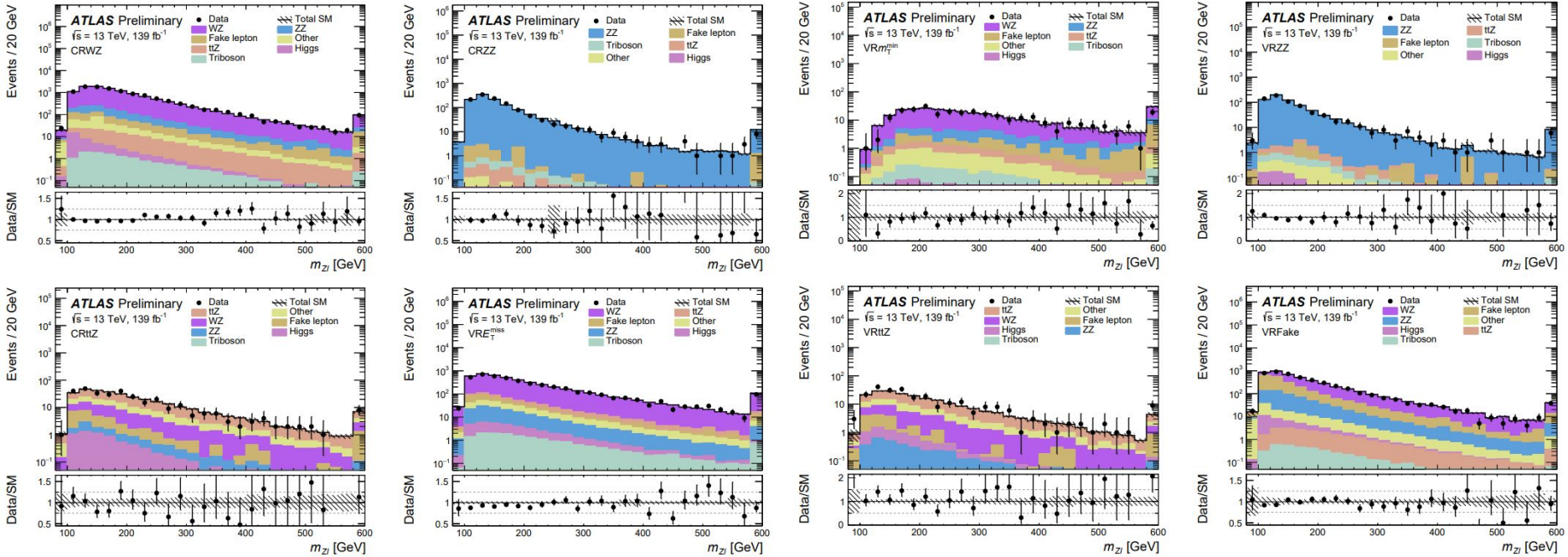

Agreement is good in all regions

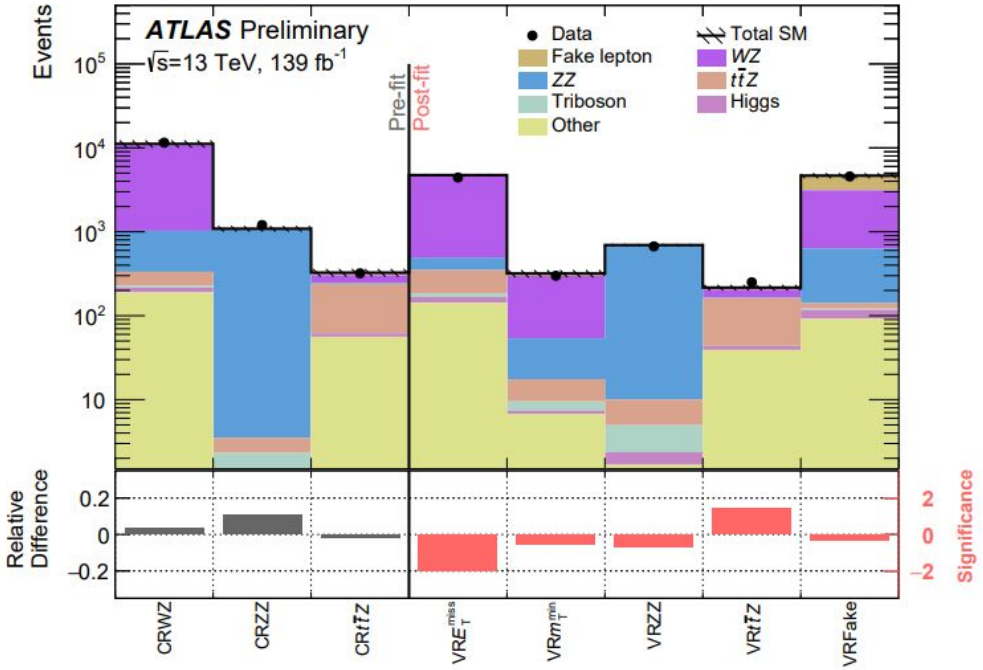

Figure 5: The observed data and the SM background expectation in the CRs (pre-fit) and VRs (post-fit). The "Other" category mostly consists of tWZ, $t\bar{t}W$, and tZ processes. The hatched bands indicate the combined theoretical, experimental, and MC statistical uncertainties. The bottom panel shows the fractional difference between the observed data and expected yields for the CRs and the significance of the difference for the VRs, computed following the profile likelihood method described in Ref. [102].

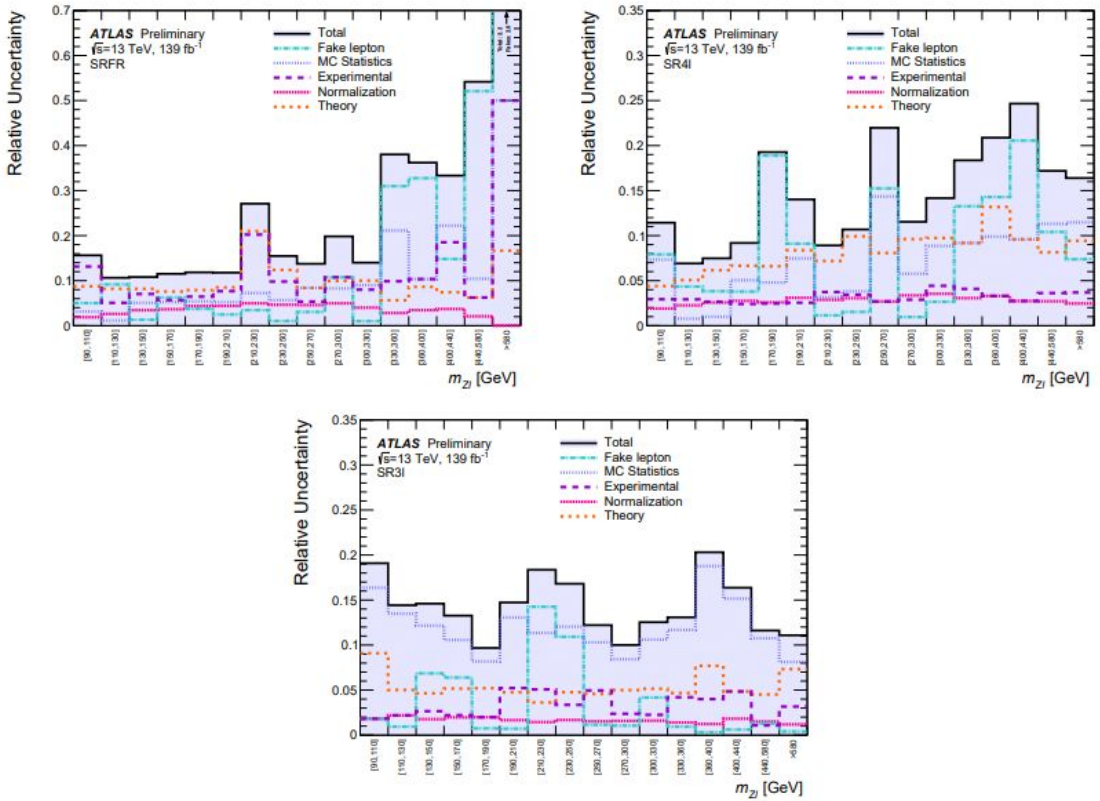

Figure 6: The relative uncertainties in the post-fit SM background prediction as a function of $m_{Z\ell}$ from the background-only fit for the (top left) SRFR, (top right) SR4ℓ, and (bottom) SR3ℓ regions. Sources of uncertainty are grouped into experimental, theoretical, and MC statistical categories. Separate categories are provided for the *fake* backgrounds and for the normalization procedure of the major WZ, ZZ, and $t\bar{t}Z$ backgrounds. The individual uncertainties can be correlated and do not necessarily add in quadrature to the total uncertainty.

- Highlighted are the overall observed yields versus the background expectations
- In general we see good agreement

Table 3: The observed yields and post-fit background expectations in SRFR, SR4ℓ, and SR3ℓ, shown inclusively and when the direct lepton from a $\tilde{\chi}_1^{\pm}/\tilde{\chi}_1^0$ decay is required to be an electron or muon. The "Other" category mostly consists of tWZ, $t\bar{t}W$, and tZ processes. Uncertainties on the background expectation include combined statistical and systematic uncertainties. The individual uncertainties may be correlated and do not necessarily add in quadrature to equal the total background uncertainty.

Region	SRFR	SRFR$_e$	SRFR$_\mu$	SR4ℓ	SR4ℓ_e	SR4ℓ_μ
Observed yield	42	15	17	89	48	41
Expected background yield	39.3 ± 3.5	13.8 ± 2.1	15.7 ± 2.6	76 ± 5	36 ± 4	38.4 ± 2.9
WZ yield	–	–	–	–	–	–
ZZ yield	19.5 ± 2.8	7.2 ± 1.7	10.4 ± 2.5	21.0 ± 1.1	9.6 ± 0.7	11.2 ± 0.8
ttZ yield	12.3 ± 2.4	2.5 ± 0.7	3.0 ± 0.7	18 ± 5	9.1 ± 3.2	8.6 ± 1.6
triboson yield	1.3 ± 0.4	0.26 ± 0.09	0.32 ± 0.12	12.2 ± 2.4	5.7 ± 1.4	5.9 ± 1.5
Higgs yield	2.7 ± 0.5	0.73 ± 0.18	1.17 ± 0.25	11.2 ± 1.7	5.2 ± 1.0	5.5 ± 1.1
Other yield	2.2 ± 0.4	0.25 ± 0.17	0.39 ± 0.16	7.9 ± 1.3	4.0 ± 0.8	3.5 ± 0.8
$fake$ yield	1.3 ± 0.7	2.9 ± 1.5	0.5 ± 0.5	6.4 ± 2.1	2.1 ± 1.1	3.6 ± 1.7

Region	SR3ℓ	SR3ℓ_e	SR3ℓ_μ
Observed yield	61	28	33
Expected background yield	55.1 ± 3.0	27.6 ± 2.4	28.0 ± 2.3
WZ yield	33.7 ± 2.1	16.6 ± 1.8	17.7 ± 1.9
ZZ yield	0.93 ± 0.23	0.11 ± 0.04	0.79 ± 0.25
ttZ yield	7.5 ± 1.6	4.1 ± 1.4	3.5 ± 0.7
triboson yield	5.6 ± 1.2	2.7 ± 0.8	2.7 ± 0.7
Higgs yield	0.51 ± 0.09	0.25 ± 0.06	0.23 ± 0.06
Other yield	4.2 ± 0.7	2.0 ± 0.4	2.0 ± 0.5
$fake$ yield	2.6 ± 1.1	1.9 ± 1.1	1.0 ± 0.8

SR3L

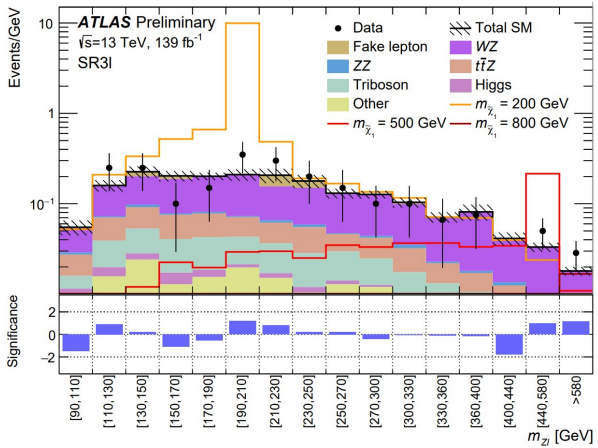

SR4L

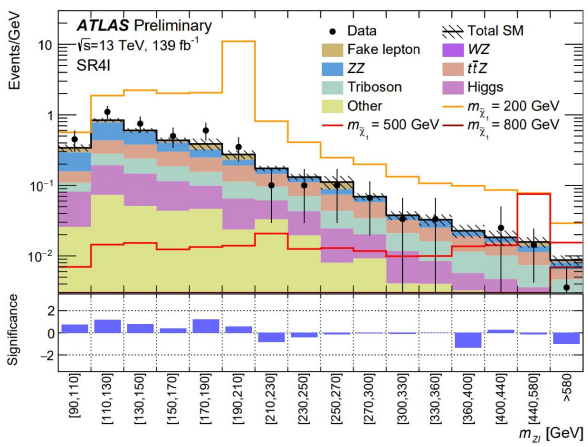

SRFR

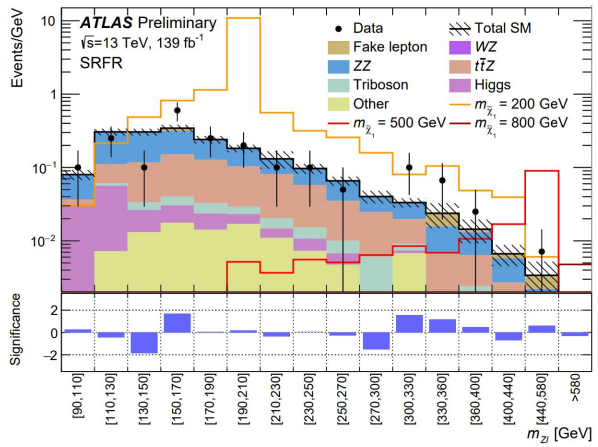

- We normalise data to the width of each bin
- The bins we chosen to maximise discovery sensitivity
- 3 benchmark signal points were chosen - 200GeV, 500GeV and 800GeV
- In general we see good agreement with some excesses and deficits, but they are not correlated in the different signal regions
- The table of yields with lepton flavor breakdown is in the backup

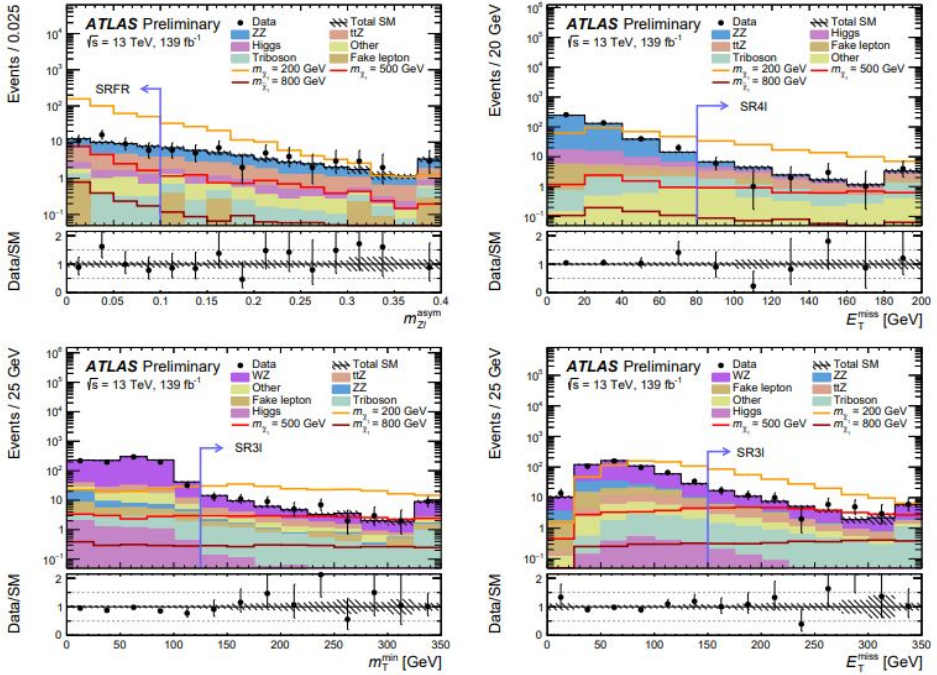

Figure 8: Example kinematic distributions in the signal regions showing the data and the post-fit background expectation, including (top left) $m_{Z\ell}^{\text{asym}}$ in SRFR, (top right) $E_{\text{T}}^{\text{miss}}$ in SR4ℓ, and (bottom left) $m_{\text{T}}^{\text{min}}$ and (bottom right) $E_{\text{T}}^{\text{miss}}$ in SR3ℓ. The fit uses all CR and SRs, and the distributions are shown inclusively in $m_{Z\ell}$. The full event selection for each of the corresponding regions is applied except for the variable shown, where the selection is indicated by a blue arrow. The first (last) bin includes underflow (overflow) events. The "Other" category mostly consists of tWZ, $t\bar{t}W$, and tZ processes. The hatched bands indicate the combined theoretical, experimental, and MC statistical uncertainties. The bottom panel shows the ratio between the data and the post-fit background prediction.

- To the right we show the results of the model independent limits
  - The number of observed events
  - The number of expected events
  - The observed limit on the visible cross section of a BSM process
  - The corresponding observed upper limit on the number of events
  - The expected upper limit on the number of BSM events
  - The p-value (and associated Z-score) for the null hypothesis
- Each bin is fit with corresponding CR + SR mZl bin
- The largest significance is 2.2 in the SRFR [150,170] bin and it highlighted in green
- Other significances above 2 sigma are highlighted in green

Region	$m_{Z\ell}$ Range	N_{obs}	N_{exp}	$\langle\epsilon\sigma\rangle^{95}_{obs}$ [fb]	S^{95}_{obs}	S^{95}_{exp}	$p(s=0)$ (Z)
SRFR	[90,110]	2	1.6 ± 0.3	0.03	4.2	$4.0^{+1.7}_{-0.7}$	0.43 (0.2)
	[110,130]	5	5.9 ± 1.0	0.04	5.7	$6.4^{+2.5}_{-1.7}$	0.50 (0.0)
	[130,150]	2	6.0 ± 1.1	0.03	4.2	$6.2^{+2.3}_{-1.5}$	0.50 (0.0)
	[150,170]	12	6.1 ± 1.1	0.10	14.2	$7.9^{+2.7}_{-1.3}$	0.01 (2.2)
	[170,190]	5	4.5 ± 0.8	0.05	6.4	$5.6^{+2.5}_{-1.3}$	0.31 (0.5)
	[190,210]	4	3.4 ± 0.6	0.04	6.1	$5.2^{+2.0}_{-1.4}$	0.26 (0.7)
	[210,230]	2	2.6 ± 1.5	0.03	4.7	$4.9^{+1.4}_{-1.4}$	0.50 (0.0)
	[230,250]	2	1.8 ± 0.3	0.03	4.6	$4.0^{+1.7}_{-0.9}$	0.42 (0.2)
	[250,270]	1	1.2 ± 0.2	0.03	3.9	$3.7^{+1.6}_{-0.7}$	0.50 (0.0)
	[270,300]	0	1.2 ± 0.3	0.03	3.6	$3.7^{+1.5}_{-0.7}$	0.50 (0.0)
	[300,330]	3	0.9 ± 0.2	0.05	6.6	$4.2^{+0.7}_{-0.5}$	0.02 (2.1)
	[330,360]	2	0.5 ± 0.2	0.04	5.6	$3.5^{+0.8}_{-0.1}$	0.03 (1.9)
	[360,400]	1	0.5 ± 0.2	0.03	4.0	$3.4^{+0.8}_{-0.1}$	0.18 (0.9)
	[400,440]	0	0.3 ± 0.1	0.03	3.7	$3.1^{+0.8}_{-0.0}$	0.50 (0.0)
	[440,580]	1	0.3 ± 0.2	0.03	4.4	$3.3^{+0.9}_{-0.1}$	0.12 (1.2)
	>580	0	$0.1^{+0.2}_{-0.1}$	0.02	3.2	$3.0^{+0.9}_{-0.0}$	0.50 (0.0)
SR4ℓ	[90,110]	9	6.1 ± 0.9	0.07	9.7	$7.1^{+2.3}_{-1.1}$	0.14 (1.1)
	[110,130]	22	15.4 ± 1.3	0.12	16.0	$10.2^{+4.2}_{-2.1}$	0.05 (1.6)
	[130,150]	15	10.9 ± 0.9	0.09	12.7	$8.5^{+3.7}_{-1.2}$	0.09 (1.3)
	[150,170]	10	7.9 ± 0.9	0.07	9.9	$7.7^{+2.8}_{-1.4}$	0.18 (0.9)
	[170,190]	12	5.9 ± 0.6	0.10	14.3	$8.5^{+3.2}_{-0.8}$	0.02 (2.0)
	[190,210]	7	4.9 ± 0.9	0.06	8.4	$6.6^{+2.2}_{-1.2}$	0.16 (1.0)
	[210,230]	2	3.2 ± 0.3	0.03	4.3	$4.8^{+2.2}_{-1.4}$	0.50 (0.0)
	[250,270]	2	2.1 ± 0.6	0.03	4.5	$4.5^{+1.9}_{-1.0}$	0.50 (0.0)
	[270,300]	2	1.9 ± 0.2	0.03	4.9	$4.8^{+1.6}_{-1.2}$	0.48 (0.1)
	[300,330]	1	1.0 ± 0.2	0.03	4.7	$4.2^{+1.6}_{-0.9}$	0.50 (0.0)
	[330,360]	1	0.9 ± 0.2	0.03	3.9	$3.6^{+1.6}_{-0.5}$	0.30 (0.5)
	[360,400]	0	0.8 ± 0.2	0.03	3.6	$3.6^{+1.1}_{-0.5}$	0.50 (0.0)
	[400,440]	1	0.6 ± 0.2	0.03	4.2	$3.2^{+1.1}_{-0.2}$	0.17 (1.0)
	[440,580]	2	2.0 ± 0.4	0.03	4.7	$4.5^{+1.7}_{-1.2}$	0.50 (0.0)
	>580	1	2.3 ± 0.5	0.03	3.5	$4.5^{+1.7}_{-1.2}$	0.50 (0.0)
SR3ℓ	[90,110]	0	1.1 ± 0.2	0.02	3.0	$3.5^{+2.2}_{-0.5}$	0.50 (0.0)
	[110,130]	5	2.8 ± 0.6	0.06	7.8	$5.7^{+1.3}_{-1.1}$	0.09 (1.3)
	[130,150]	5	4.1 ± 0.8	0.05	6.8	$5.7^{+2.3}_{-1.1}$	0.27 (0.6)
	[150,170]	2	4.0 ± 0.7	0.03	3.8	$5.3^{+2.2}_{-1.5}$	0.50 (0.0)
	[170,190]	3	3.9 ± 0.5	0.04	4.9	$5.4^{+2.2}_{-1.7}$	0.50 (0.0)
	[190,210]	7	3.7 ± 0.8	0.07	9.1	$6.2^{+1.8}_{-1.6}$	0.12 (1.2)
	[210,230]	6	3.5 ± 0.9	0.06	8.9	$6.2^{+2.0}_{-1.8}$	0.09 (1.4)
	[230,250]	4	3.3 ± 0.7	0.04	6.0	$5.4^{+1.8}_{-1.2}$	0.29 (0.6)
	[250,270]	3	2.5 ± 0.4	0.04	5.4	$4.8^{+1.8}_{-1.3}$	0.37 (0.3)
	[270,300]	3	3.7 ± 0.5	0.04	5.1	$5.4^{+2.0}_{-1.7}$	0.50 (0.0)
	[300,330]	3	3.0 ± 0.5	0.04	5.0	$4.9^{+2.1}_{-1.2}$	0.50 (0.0)
	[330,360]	2	2.1 ± 0.4	0.03	4.7	$4.4^{+1.7}_{-1.1}$	0.50 (0.0)
	[360,400]	3	3.2 ± 0.9	0.04	5.4	$5.6^{+2.0}_{-1.8}$	0.50 (0.0)
	[400,440]	0	1.7 ± 0.3	0.02	3.0	$4.0^{+1.2}_{-0.6}$	0.50 (0.0)
	[440,580]	7	4.3 ± 0.7	0.06	8.7	$6.3^{+1.5}_{-1.6}$	0.11 (1.2)
	>580	8	4.6 ± 0.7	0.07	10.0	$6.6^{+2.2}_{-1.6}$	0.08 (1.4)

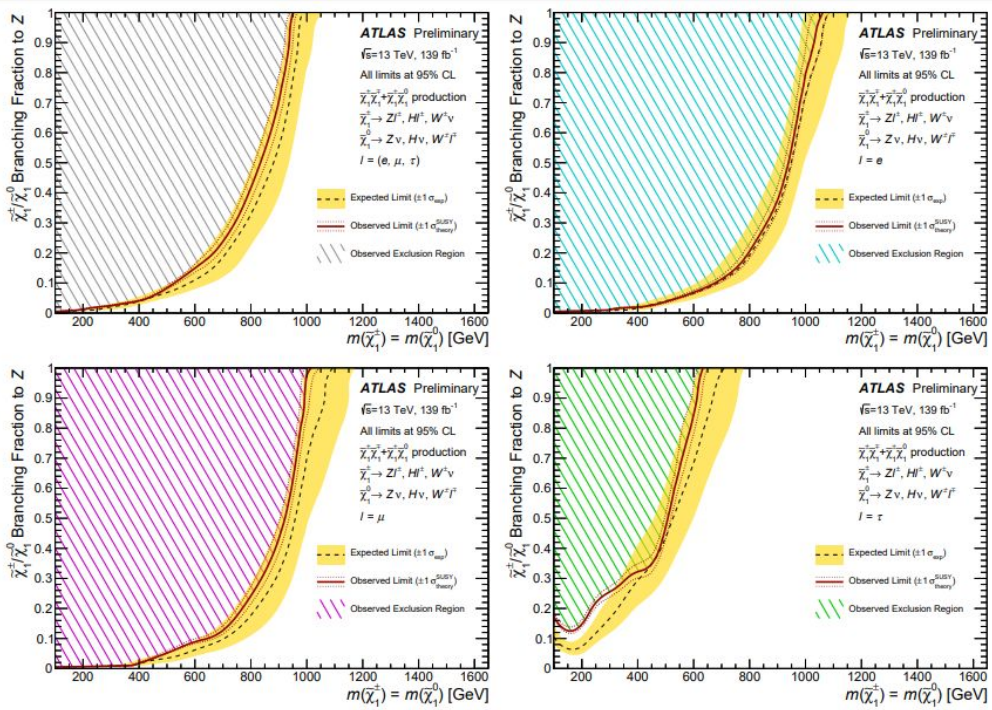

Figure 9: Exclusion curves for the simplified model of $\tilde{\chi}_1^{\pm}\tilde{\chi}_1^{\mp} + \tilde{\chi}_1^{\pm}\tilde{\chi}_1^0$ pair-production as a function of $\tilde{\chi}_1^{\pm}/\tilde{\chi}_1^0$ mass and branching fraction to Z bosons. Curves are derived separately when requiring that the charged-lepton decays of the $\tilde{\chi}_1^{\pm}/\tilde{\chi}_1^0$ are to (top left) any lepton with equal probability, (top right) an electron only, (bottom left) a muon only, or (bottom right) a τ lepton only. The expected 95% CL exclusion (dashed black line) is shown with $\pm 1\ \sigma_{\text{exp}}$ (yellow band) from systematic and statistical uncertainties on the expected yields. The observed 95% CL exclusion (solid red line) is shown with the $\pm 1\ \sigma_{\text{theory}}^{\text{SUSY}}$ (dotted red line) from signal cross section uncertainties on the signal models. The phase-space excluded by the search is shown in the shaded color. The sum of the $\tilde{\chi}_1^{\pm}/\tilde{\chi}_1^0$ branching fractions to W, Z, and Higgs bosons is unity for each point, and the branching fractions to W and Higgs bosons are chosen so as to be equal everywhere.

9 Conclusion

This paper presents a search for the production of wino-type $\tilde{\chi}_1^{\pm}\tilde{\chi}_1^{\mp}$ and $\tilde{\chi}_1^{\pm}\tilde{\chi}_1^{0}$ processes where each $\tilde{\chi}_1^{\pm}/\tilde{\chi}_1^{0}$ decays via an RPV coupling to a W, Z, or Higgs boson and a lepton. The dataset corresponds to an integrated luminosity of 139 fb^{-1} of proton–proton collision data produced at a center-of-mass energy of $\sqrt{s} = 13$ TeV and collected by the ATLAS experiment between 2015 and 2018. This new search primarily targets the three-lepton decay of a $\tilde{\chi}_1^{\pm}$ and is the first ATLAS analysis using $\sqrt{s} = 13$ TeV data to search for a mass resonance in the $m_{Z\ell}$ spectrum. Three signal regions are defined that target events with three or more leptons and missing transverse energy or with two fully-reconstructed $\tilde{\chi}_1^{\pm}/\tilde{\chi}_1^{0}$ decays. The observed event yields are found to be in agreement with Standard Model expectations, with no significant excess seen in the $m_{Z\ell}$ distributions of the signal regions.

Model-independent limits are set at a 95% confidence level for each $m_{Z\ell}$ bin in each signal region. The largest excess of data over the expectation in the 48 model-independent regions is found to be 2.2 σ. No trend is seen in the distribution of data excesses in $m_{Z\ell}$ bins between the three signal regions. Model-specific lower limits are also set on the $\tilde{\chi}_1^{\pm}/\tilde{\chi}_1^{0}$ masses for various decay branching fractions into electron, muon, or τ leptons and into W, Z, or Higgs bosons, probing sensitivity to the neutrino mass hierarchy and the MSSM parameters of the $B - L$ RPV theory. For scenarios with large $\tilde{\chi}_1^{\pm}/\tilde{\chi}_1^{0}$ branching fractions to Z bosons, lower limits on the $\tilde{\chi}_1^{\pm}/\tilde{\chi}_1^{0}$ masses are set at 625 GeV, 1000 GeV, and 1050 GeV for 100% branching fractions to τ leptons, muons, and electrons, respectively.

2L COMPRESSED ADDITIONAL MATERIAL

TABLE I. Simulated SM background processes. The PDF set refers to that used for the matrix element.

Process	Matrix element	Parton shower	PDF set	Cross section
V + jets	SHERPA2.2.1		NNPDF 3.0 NNLO [84]	NNLO [85]
VV	SHERPA2.2.1/2.2.2		NNPDF 3.0 NNLO	Generator NLO
Triboson	SHERPA2.2.1		NNPDF 3.0 NNLO	Generator LO, NLO
h (ggF)	POWHEG-BOX	PYTHIA8.212	NLO CTEQ6L1 [86]	N^3LO [87]
h (VBF)	POWHEG-BOX	PYTHIA8.186	NLO CTEQ6L1 [86]	NNLO + NLO [87]
$h + W/Z$	PYTHIA8.186		NNPDF 2.3 LO [54]	NNLO + NLO [87]
$h + t\bar{t}$	MG5_aMC@NLO2.2.3	PYTHIA8.210	NNPDF 2.3 LO	NLO [87]
$t\bar{t}$	POWHEG-BOX	PYTHIA8.230	NNPDF 2.3 LO	NNLO + NNLL [88–92]
t (s channel)	POWHEG-BOX	PYTHIA8.230	NNPDF 2.3 LO	NNLO + NNLL [93]
t (t channel)	POWHEG-BOX	PYTHIA8.230	NNPDF 2.3 LO	NNLO + NNLL [77,94]
$t + W$	POWHEG-BOX	PYTHIA8.230	NNPDF 2.3 LO	NNLO + NNLL [95]
$t + Z$	MG5_aMC@NLO2.3.3	PYTHIA8.212	NNPDF 2.3 LO	NLO [53]
$t\bar{t}WW$	MG5_aMC@NLO2.2.2	PYTHIA8.186	NNPDF 2.3 LO	NLO [53]
$t\bar{t} + Z/W/\gamma^*$	MG5_aMC@NLO2.3.3	PYTHIA8.210/8.212	NNPDF 2.3 LO	NLO [87]
$t + WZ$	MG5_aMC@NLO2.3.3	PYTHIA8.212	NNPDF 2.3 LO	NLO [53]
$t + t\bar{t}$	MG5_aMC@NLO2.2.2	PYTHIA8.186	NNPDF 2.3 LO	LO [53]
$tt\bar{t}\bar{t}$	MG5_aMC@NLO2.2.2	PYTHIA8.186	NNPDF 2.3 LO	NLO [53]

Events were selected with a $E_{\mathrm{T}}^{\mathrm{miss}}$ trigger, employing varied trigger thresholds as a function of the data-taking periods. The trigger is > 95% efficient for offline $E_{\mathrm{T}}^{\mathrm{miss}}$ values above 200 GeV for all periods. The dataset used corresponds to 139 fb^{-1} of $\sqrt{s}$ = 13 TeV pp collision data, where the uncertainty in the integrated luminosity is 1.7% [50], obtained using the LUCID-2 detector [51] for the primary luminosity measurements. The average number of interactions per bunch-crossing was 33.7.

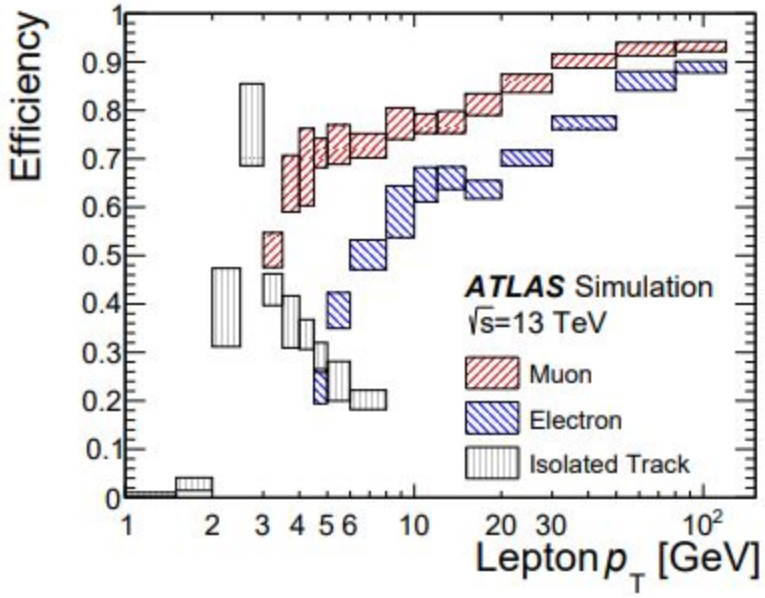

Figure 3: Signal lepton efficiencies for electrons, muons, and isolated tracks in a mix of slepton and higgsino samples. Combined reconstruction, identification, isolation and vertex association efficiencies are shown for leptons within detector acceptance, and with lepton p_T within a factor of 3 of $\Delta m(\tilde{\ell}, \tilde{\chi}_1^0)$ for sleptons or of $\Delta m(\tilde{\chi}_2^0, \tilde{\chi}_1^0)/2$ for higgsinos. The efficiencies for isolated tracks include track reconstruction and vertex association efficiencies [112], as well as the efficiencies for track–lepton matching and track isolation, which are specific to this search. Scale factors are applied to match reconstruction efficiencies in data. The average number of interactions per crossing in the MC samples is 33.7; the number of pileup interactions match the distribution in data in spread and mean value. Uncertainty bands represent the range of efficiencies observed across all signal samples used for the given p_T bin.

Recursive Jigsaw Reconstruction

- Recursive Jigsaw Reconstruction allows us to define a topology of an event
- We define an ISR system, which is kicking off the sparticle system.
- The sparticle system then decays into visible and invisible components
- We can construct many useful variables, two of which are RISR and MTS.
- RISR is the momentum of the invisible system along the axis of the ISR kick, in units of the ISR kick
- MTS is the transverse mass of the sparticle system
- To the right we show RISR vs mll
- RISR peaks heavily for highly compressed scenarios
- The red line highlights our selection in this analysis.

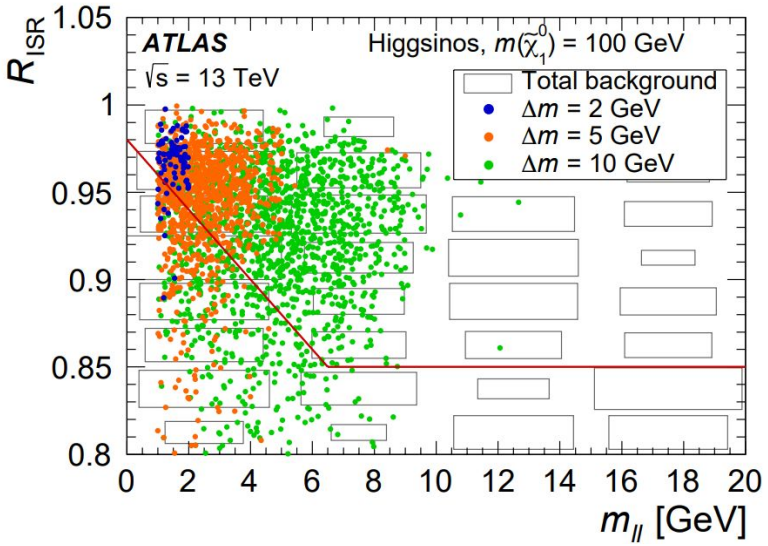

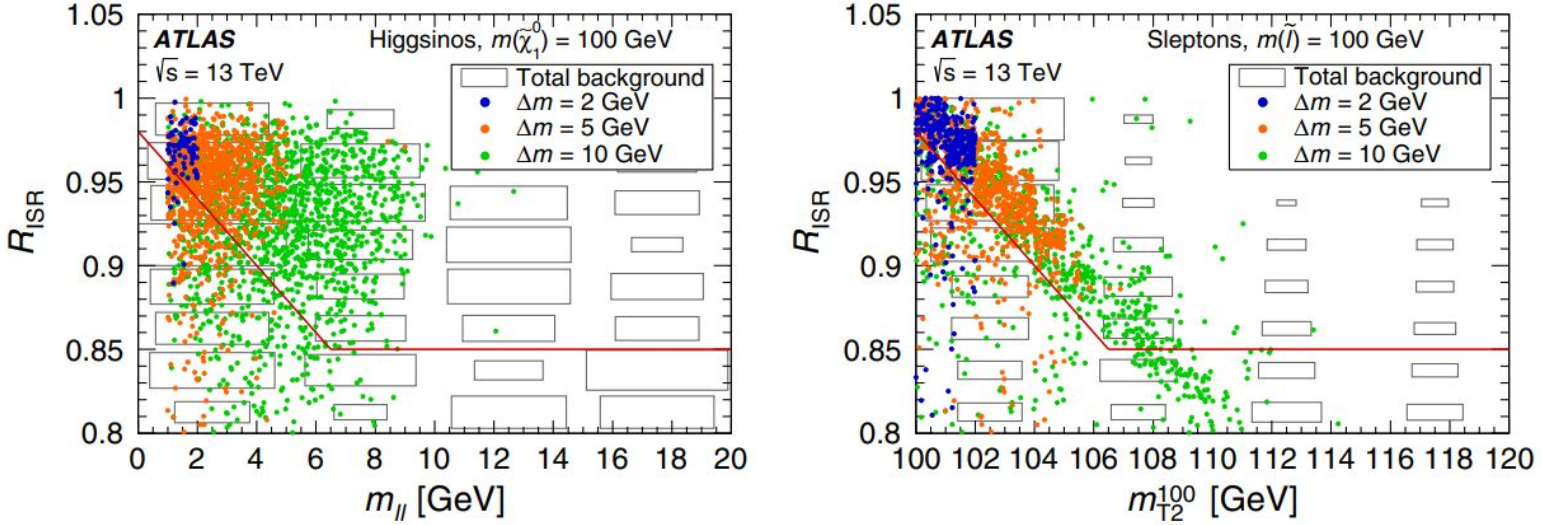

FIG. 4. Distributions of R_{ISR}, the ratio of the $E_{\mathrm{T}}^{\mathrm{miss}}$ to the transverse momentum of the hadronic ISR activity, for the electroweakino (left) and slepton (right) high-$E_{\mathrm{T}}^{\mathrm{miss}}$ SRs. Distributions are shown after applying all signal selection criteria except those on R_{ISR}. The solid red line indicates the requirement applied in the signal region; events in the region below the red line are rejected. Representative benchmark signals for the Higgsino (left) and slepton (right) simplified models are shown as circles. The gray rectangular boxes show the distribution of the total background prediction, which is primarily composed of top-like processes, diboson processes, and events with fake/nonprompt leptons. Regions at larger $m_{\ell\ell}$ and m_{T2} are not populated by the representative signals shown here, but are useful probes of less-compressed signal models.

TABLE II. Preselection requirements applied to all events entering into electroweakino, slepton, and VBF search regions. Requirements marked with † are not applied to VBF search regions. Requirements on jets are applied to VBF jets (satisfying $|\eta| < 4.5$) in the VBF channel.

	Preselection requirements	
Variable	2ℓ	$1\ell 1T$
Number of leptons (tracks)	=2 leptons	=1 lepton and ≥1 track
Lepton p_{T} [GeV]	$p_{\mathrm{T}}^{\ell_1} > 5$	$p_{\mathrm{T}}^{\ell} < 10$
$\Delta R_{\ell\ell}$	$\Delta R_{ee} > 0.30$, $\Delta R_{\mu\mu} > 0.05$, $\Delta R_{e\mu} > 0.2$	$0.05 < \Delta R_{\ell\mathrm{track}} < 1.5$
Lepton (track) charge and flavor	$e^{\pm}e^{\mp}$ or $\mu^{\pm}\mu^{\mp}$	$e^{\pm}e^{\mp}$ or $\mu^{\pm}\mu^{\mp}$
Lepton (track) invariant mass [GeV]	$3 < m_{ee} < 60$, $1 < m_{\mu\mu} < 60$	$0.5 < m_{\ell\mathrm{track}} < 5$
J/ψ invariant mass [GeV]	veto $3 < m_{\ell\ell} < 3.2$	veto $3 < m_{\ell\mathrm{track}} < 3.2$
$m_{\tau\tau}$ [GeV]	<0 or >160	no requirement
$E_{\mathrm{T}}^{\mathrm{miss}}$ [GeV]	>120	>120
Number of jets	≥1	≥1
Number of b-tagged jets	= 0	no requirement
Leading jet p_{T} [GeV]	≥100	≥100
$\min(\Delta\phi(\text{any jet}, \mathbf{p}_{\mathrm{T}}^{\mathrm{miss}}))$	>0.4	>0.4
$\Delta\phi(j_1, \mathbf{p}_{\mathrm{T}}^{\mathrm{miss}})^{\dagger}$	≥2.0	≥2.0

TABLE III. Requirements applied to events entering into the four signal regions used for electroweakino searches. The $1\ell 1T$ preselection requirements from Table II are implied for SR-E-$1\ell 1T$, while the 2ℓ ones are implied for the other SRs.

	Electroweakino SR requirements			
Variable	SR-E-low	SR-E-med	SR-E-high	SR-E-$1\ell 1T$
$E_{\mathrm{T}}^{\mathrm{miss}}$ [GeV]	[120, 200]	[120, 200]	>200	>200
$E_{\mathrm{T}}^{\mathrm{miss}}/H_{\mathrm{T}}^{\mathrm{lep}}$	<10	>10	···	>30
$\Delta\phi(\mathrm{lep}, \mathbf{p}_{\mathrm{T}}^{\mathrm{miss}})$	···	···	···	<1.0
Lepton or track p_{T} [GeV]	$p_{\mathrm{T}}^{\ell_2} > 5 + m_{\ell\ell}/4$	···	$p_{\mathrm{T}}^{\ell_2} > \min(10, 2 + m_{\ell\ell}/3)$	$p_{\mathrm{T}}^{\mathrm{track}} < 5$
$M_{\mathrm{T}}^{\mathrm{S}}$ [GeV]	···	<50	···	···
$m_{\mathrm{T}}^{\ell_1}$ [GeV]	[10, 60]	···	<60	···
R_{ISR}	[0.8, 1.0]	···	$[\max(0.85, 0.98 - 0.02 \times m_{\ell\ell}), 1.0]$	···

TABLE IV. Requirements applied to all events entering into signal regions used for searches for electroweakinos produced through VBF. The 2ℓ preselection requirements from Table II are implied.

Variable	VBF SR requirements
$m_{\ell\ell}$ [GeV]	<40
Number of jets	≥2
$p_{\mathrm{T}}^{j_2}$ [GeV]	>40
$E_{\mathrm{T}}^{\mathrm{miss}}$ [GeV]	>150
$E_{\mathrm{T}}^{\mathrm{miss}}/H_{\mathrm{T}}^{\mathrm{lep}}$	>2
$p_{\mathrm{T}}^{\ell_2}$ [GeV]	$>\min(10, 2 + m_{\ell\ell}/3)$
$m_{\mathrm{T}}^{\ell_1}$ [GeV]	<60
R_{VBF}	$[\max(0.6, 0.92 - m_{\ell\ell}/60), 1.0]$
$\eta_{j_1} \cdot \eta_{j_2}$	<0
m_{jj} [GeV]	>400
$\Delta\eta_{jj}$	>2

	SR-VBF-low	SR-VBF-high
$\Delta\eta_{jj}$	<4	>4

TABLE V. Requirements applied to all events entering into signal regions used for slepton searches. The 2ℓ preselection requirements from Table II are implied.

	Slepton SR requirements	
Variable	SR-S-low	SR-S-high
$E_{\mathrm{T}}^{\mathrm{miss}}$ [GeV]	[150, 200]	>200
m_{T2}^{100} [GeV]	<140	<140
$p_{\mathrm{T}}^{\ell_2}$ [GeV]	$> \min(15, 7.5 + 0.75 \times (m_{\mathrm{T2}} - 100))$	$> \min(20, 2.5 + 2.5 \times (m_{\mathrm{T2}} - 100))$
R_{ISR}	[0.8, 1.0]	$[\max(0.85, 0.98 - 0.02 \times (m_{\mathrm{T2}} - 100)), 1.0]$

$$m_{\mathrm{T2}}^{m_\chi}(\mathbf{p}_{\mathrm{T}}^{\ell_1}, \mathbf{p}_{\mathrm{T}}^{\ell_2}, \mathbf{p}_{\mathrm{T}}^{\mathrm{miss}}) = \min_{\mathbf{q}_{\mathrm{T}}}(\max[m_{\mathrm{T}}(\mathbf{p}_{\mathrm{T}}^{\ell_1}, \mathbf{q}_{\mathrm{T}}, m_\chi), m_{\mathrm{T}}(\mathbf{p}_{\mathrm{T}}^{\ell_2}, \mathbf{p}_{\mathrm{T}}^{\mathrm{miss}} - \mathbf{q}_{\mathrm{T}}, m_\chi)]),$$

$$m_{\mathrm{T}}(\mathbf{p}_{\mathrm{T}}, \mathbf{q}_{\mathrm{T}}, m_\chi) = \sqrt{m_\ell^2 + m_\chi^2 + 2\left(\sqrt{p_{\mathrm{T}}^2 + m_\ell^2}\sqrt{q_{\mathrm{T}}^2 + m_\chi^2} - \mathbf{p}_{\mathrm{T}} \cdot \mathbf{q}_{\mathrm{T}}\right)}.$$

For signal events with slepton mass $m(\tilde{\ell})$ and LSP mass $m(\tilde{\chi}_1^0)$, the values of $m_{\mathrm{T2}}{}^{m_\chi}$ are bounded from above by $m(\tilde{\ell})$ when m_χ is equal to $m(\tilde{\chi}_1^0)$. The stransverse mass with $m_\chi = 100$ GeV, denoted m_{T2}^{100}, is used in this paper. The chosen value of 100 GeV is based on the expected LSP masses of the signals studied. The distribution of m_{T2}^{100} does not vary significantly for the signals considered in which $m(\tilde{\chi}_1^0) \neq 100$ GeV.

TABLE VI. Definition of control ("CR" prefix) and validation ("VR" prefix) regions used for background estimation in the electroweakino search, presented relative to the definitions of the corresponding signal regions SR-E-high, SR-E-med, and SR-E-low. The 2ℓ preselection criteria from Table II and selection criteria from Table III are implied, unless specified otherwise.

Region	SR orthogonality	Lepton flavor	Additional requirements
CRtop-E-high	$N^{20}_{b\text{-jet}} \geq 1$	$ee + \mu\mu + e\mu + \mu e$	$R_{\text{ISR}} \in [0.7, 1.0]$, $m_{\text{T}}^{\ell_1}$ removed
CRtop-E-low			$E_{\text{T}}^{\text{miss}}/H_{\text{T}}^{\text{lep}}$ and $m_{\text{T}}^{\ell_1}$ removed
CRtau-E-high	$m_{\tau\tau} \in [60, 120]$ GeV	$ee + \mu\mu + e\mu + \mu e$	$R_{\text{ISR}} \in [0.7, 1.0]$, $m_{\text{T}}^{\ell_1}$ removed
CRtau-E-low			$R_{\text{ISR}} \in [0.6, 1.0]$, $m_{\text{T}}^{\ell_1}$ removed
VRtau-E-med			...
CRVV-E-high	$R_{\text{ISR}} \in [0.7, 0.85]$	$ee + \mu\mu + e\mu + \mu e$	$m_{\text{T}}^{\ell_1}$ removed
CRVV-E-low	$R_{\text{ISR}} \in [0.6, 0.8]$		$m_{\text{T}}^{\ell_1} > 30$ GeV, $N_{\text{jets}} \in [1, 2]$, $E_{\text{T}}^{\text{miss}}/H_{\text{T}}^{\text{lep}}$ removed
VRSS-E-high	Same sign $\ell^{\pm}\ell^{\pm}$	$ee + \mu e, \mu\mu + e\mu$	$R_{\text{ISR}} \in [0.7, 1.0]$, $m_{\text{T}}^{\ell_1}$ and $p_{\text{T}}^{\ell_2}$ removed
VRSS–E–low			$E_{\text{T}}^{\text{miss}}/H_{\text{T}}^{\text{lep}}$, $m_{\text{T}}^{\ell_1}$ and $p_{\text{T}}^{\ell_2}$ removed
VRSS-E-med			...
VRDF-E-high	$e\mu + \mu e$	$e\mu + \mu e$	...
VRDF-E-low			...
VRDF-E-med			...

TABLE VII. Definition of control ("CR" prefix) and validation ("VR" prefix) regions used for background estimation in the search for electroweakinos produced through VBF, presented relative to the definitions of the corresponding signal regions SR-VBF-high and SR-VBF-low. The 2ℓ preselection criteria from Table II and selection criteria from Table IV are implied, unless specified otherwise.

Region	SR orthogonality	Lepton flavor	Additional requirements
CRtop-VBF	$N^{20}_{b\text{-jet}} \geq 1$	$ee + \mu\mu + e\mu + \mu e$	R_{VBF} and $m_{\text{T}}^{\ell_1}$ removed
CRtau-VBF	$m_{\tau\tau} \in [60, 120]$ GeV	$ee + \mu\mu + e\mu + \mu e$	$E_{\text{T}}^{\text{miss}}/H_{\text{T}}^{\text{lep}} \in [2, 10]$, R_{VBF} and $m_{\text{T}}^{\ell_1}$ removed
VRSS-VBF	Same sign $\ell^{\pm}\ell^{\pm}$	$ee + \mu e, \mu\mu + e\mu$	R_{VBF}, $m_{\text{T}}^{\ell_1}$ and $p_{\text{T}}^{\ell_2}$ removed
VRDF-VBF-low	$e\mu + \mu e$	$e\mu + \mu e$	...
VRDF-VBF-high	$e\mu + \mu e$	$e\mu + \mu e$	...

TABLE VIII. Definition of control ("CR" prefix) and validation ("VR" prefix) regions used for background estimation in the slepton search, presented relative to the definitions of the corresponding signal regions SR-S-high and SR-S-low. The 2ℓ preselection criteria from Table II and selection criteria from Table V are implied, unless specified otherwise.

Region	SR orthogonality	Lepton flavor	Additional requirements
CRtop-S-high	$N^{20}_{b\text{-jet}} \geq 1$	$ee + \mu\mu + e\mu + \mu e$	$R_{\text{ISR}} \in [0.7, 1.0]$
CRtop-S-low			...
CRtau-S-high	$m_{\tau\tau} \in [60, 120]$ GeV	$ee + \mu\mu + e\mu + \mu e$	$R_{\text{ISR}} \in [0.7, 1.0]$
CRtau-S-low			$R_{\text{ISR}} \in [0.6, 1.0]$
CRVV-S-high	$R_{\text{ISR}} \in [0.7, 0.85]$	$ee + \mu\mu + e\mu + \mu e$	...
CRVV-S-low	$R_{\text{ISR}} \in [0.6, 0.8]$		$m_{\text{T}}^{\ell_1} > 30$, $N_{\text{jets}} \in [1, 2]$
VRSS-S-high	Same sign $\ell^{\pm}\ell^{\pm}$	$ee + \mu e, \mu\mu + e\mu$	$R_{\text{ISR}} \in [0.7, 1.0]$, $p_{\text{T}}^{\ell_2}$ removed
VRSS-S-low			$p_{\text{T}}^{\ell_2}$ removed
VRDF-S-high	$e\mu + \mu e$	$e\mu + \mu e$	...
VRDF-S-low			...

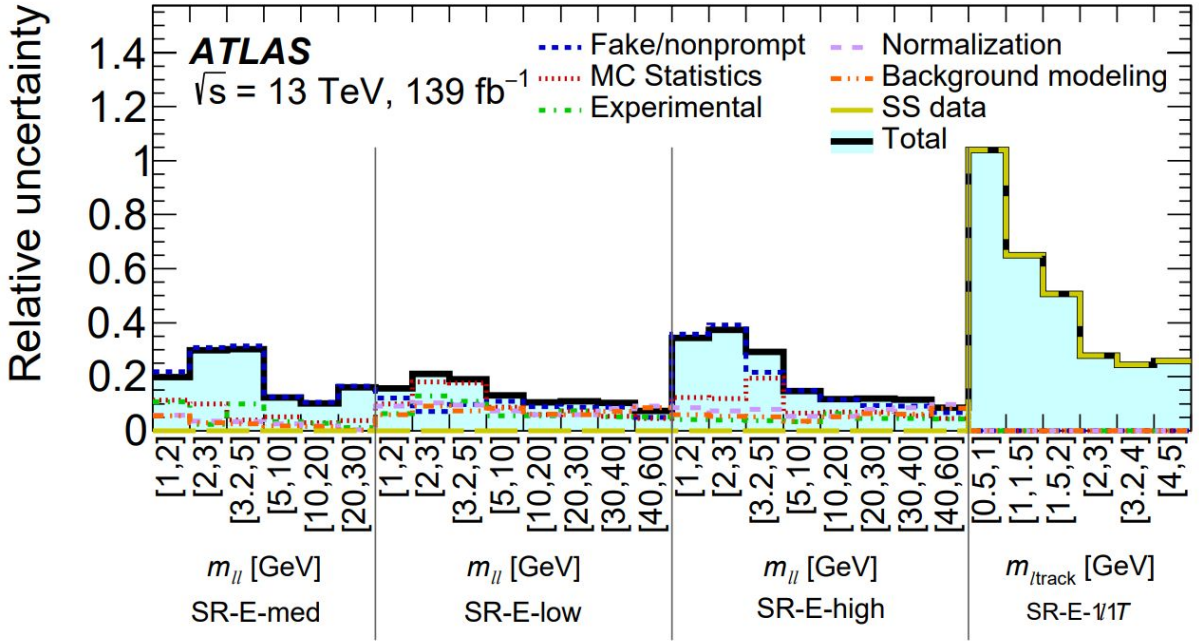

Figure plots continue next slides

Figure 5: The relative systematic uncertainties in the fitted SM background as obtained from CR+SR background-only fits for the electroweakino SRs (top), VBF SRs (middle), and slepton SRs (bottom). The uncertainty in the *SS data* includes a statistical component due to the size of the SS data sample used to estimate the background in the SR-E-1ℓ1T region, and a systematic component from the SS–OS extrapolation. The *MC Statistics* uncertainty originates from the limited size of the MC samples used to model the irreducible background contributions. The *Normalization* uncertainty arises from the use of CRs to normalize the contributions of $t\bar{t}/tW$, $Z^{(*)}/\gamma^*(\rightarrow \tau\tau)$ + jets and WW/WZ backgrounds, while *Background modeling* includes the different sources of theoretical modeling uncertainties in the $m_{\ell\ell}$ or $m_{\tau 2}^{100}$ lineshapes for the irreducible backgrounds. All sources of uncertainty affecting the FNP background estimate are included under *Fake/nonprompt*. The uncertainties arising from the reconstruction and selection of signal leptons, jets and $E_{\mathrm{T}}^{\mathrm{miss}}$ are included under the *Experimental* category. The individual uncertainties can be correlated and do not necessarily add up in quadrature to the total uncertainty.

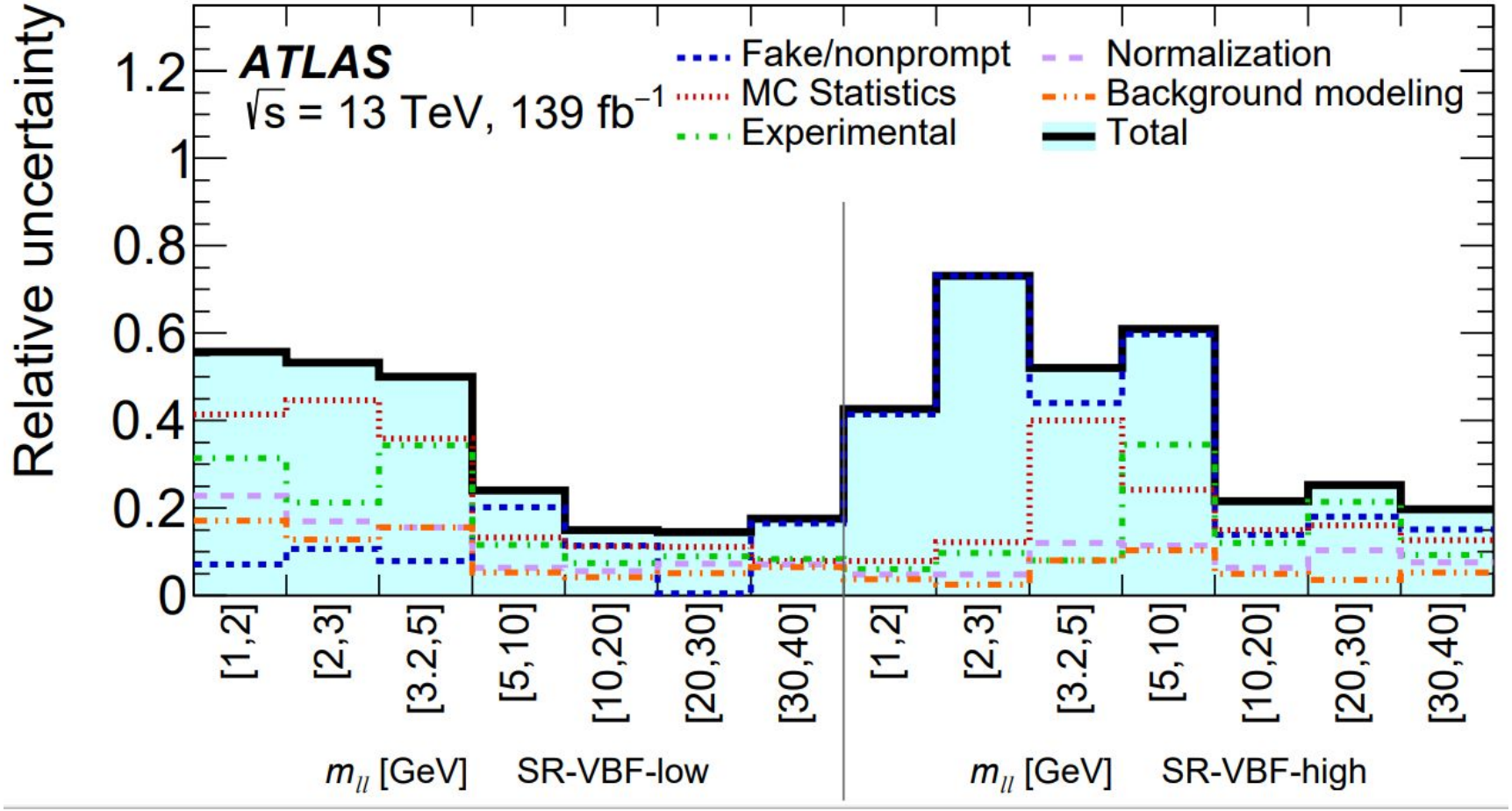
ATLAS
√s = 13 TeV, 139 fb−1
Fake/nonprompt
MC Statistics
Experimental
Normalization
Background modeling
Total
Relative uncertainty
1.2
1
0.8
0.6
0.4
0.2
0
[1,2]
[2,3]
[3.2,5]
[5,10]
[10,20]
[20,30]
[30,40]
[1,2]
[2,3]
[3.2,5]
[5,10]
[10,20]
[20,30]
[30,40]
m_{ll} [GeV]
SR-VBF-low
m_{ll} [GeV]
SR-VBF-high

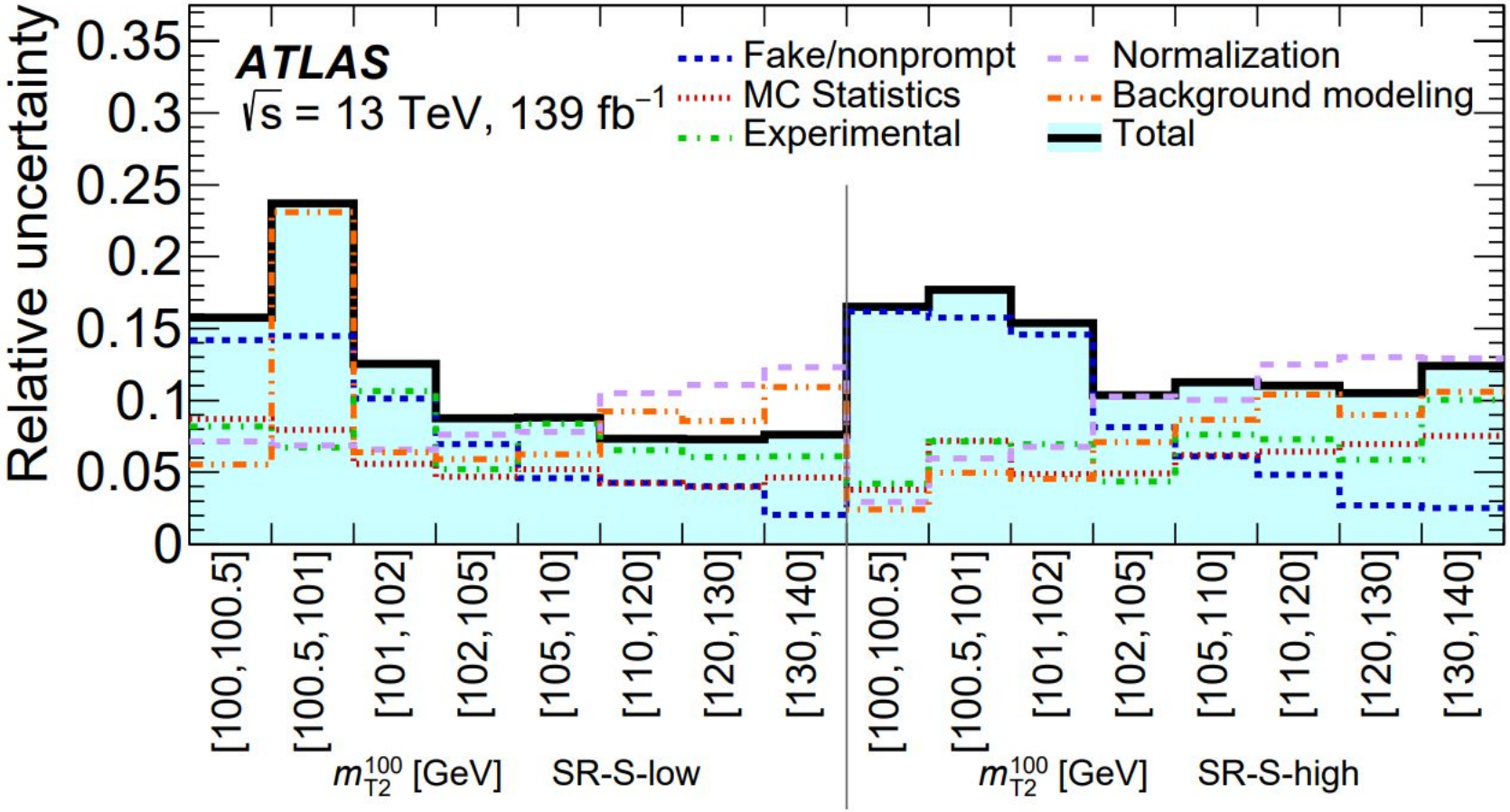
ATLAS
√s = 13 TeV, 139 fb−1
Fake/nonprompt
MC Statistics
Experimental
Normalization
Background modeling
Total
Relative uncertainty
0.35
0.3
0.25
0.2
0.15
0.1
0.05
0
[100,100.5]
[100.5,101]
[101,102]
[102,105]
[105,110]
[110,120]
[120,130]
[130,140]
m_{T2}^{100} [GeV] SR-S-low
m_{T2}^{100} [GeV] SR-S-high

Table 9: Normalization factors obtained from a background-only fit of the CRs defined for electroweakino, slepton and VBF searches. The uncertainties include statistical and systematic contributions combined.

		Normalization Parameters		
Backgrounds	$E_{\mathrm{T}}^{\mathrm{miss}}$ region	electroweakino	slepton	VBF
$t\bar{t}/Wt$	high	1.08 ± 0.20	1.05 ± 0.20	1.04 ± 0.04
	low	1.08 ± 0.18	1.09 ± 0.19	
$Z^{(*)}/\gamma^{*}(\rightarrow \tau\tau)$ + jets	high	0.96 ± 0.14	0.80 ± 0.17	0.97 ± 0.13
	low	1.02 ± 0.15	1.08 ± 0.17	
VV	high	0.89 ± 0.27	0.85 ± 0.28	–
	low	0.69 ± 0.22	0.71 ± 0.23	

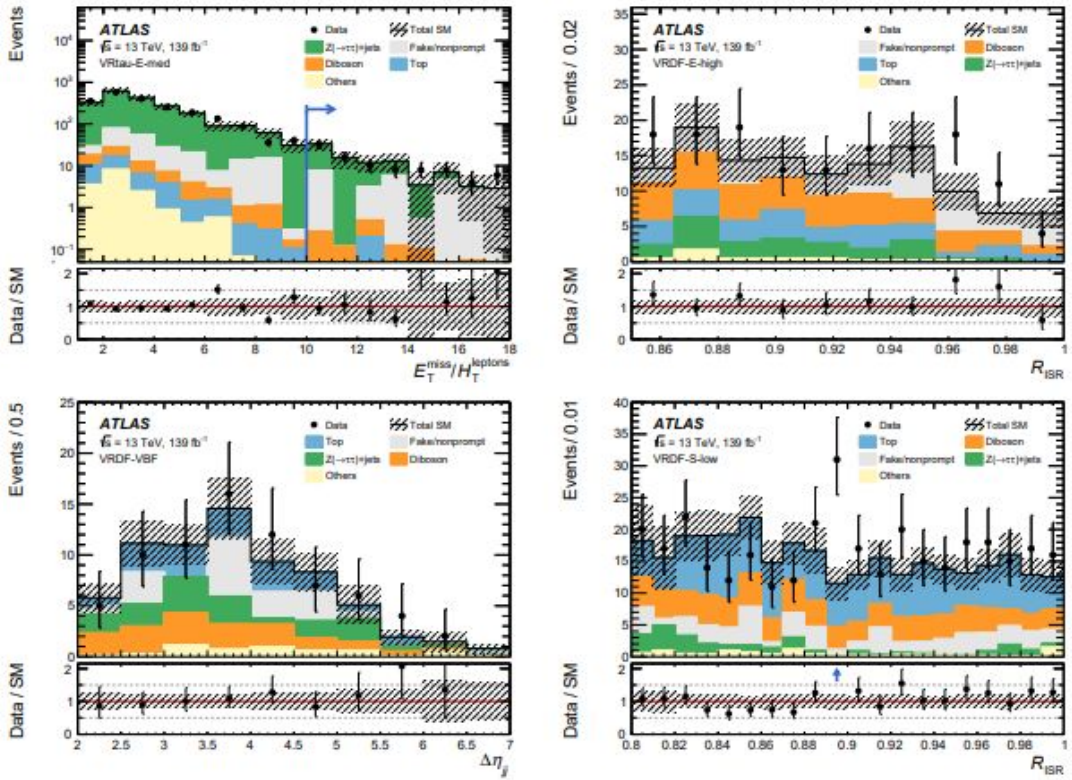

Figure 8: Examples of kinematic distributions after the background-only fit of the CRs showing the data as well as the expected background in the validation regions VRtau–E–med (top left), VRDF–E–high (top right), VRDF–VBF, including both VRDF-VBF-high and VRDF-VBF-low (bottom left) and VRDF–S–low (bottom right). The full event selection of the corresponding regions is applied, except for distributions showing blue arrows, where the requirement on the variable being plotted is removed and indicated by the arrows in the distributions instead. The first (last) bin includes underflow (overflow). The uncertainty bands plotted include all statistical and systematic uncertainties.

Electroweak Validation Regions

- The main backgrounds are tt, tW, WW/WZ + Z->tautau
- CR + VR definitions in backup
- Right: post fit results for Different Flavor VRs
- Significances extracted via profiled likelihood approach
- All deviations within 2 sigma
- Good agreement across all bins

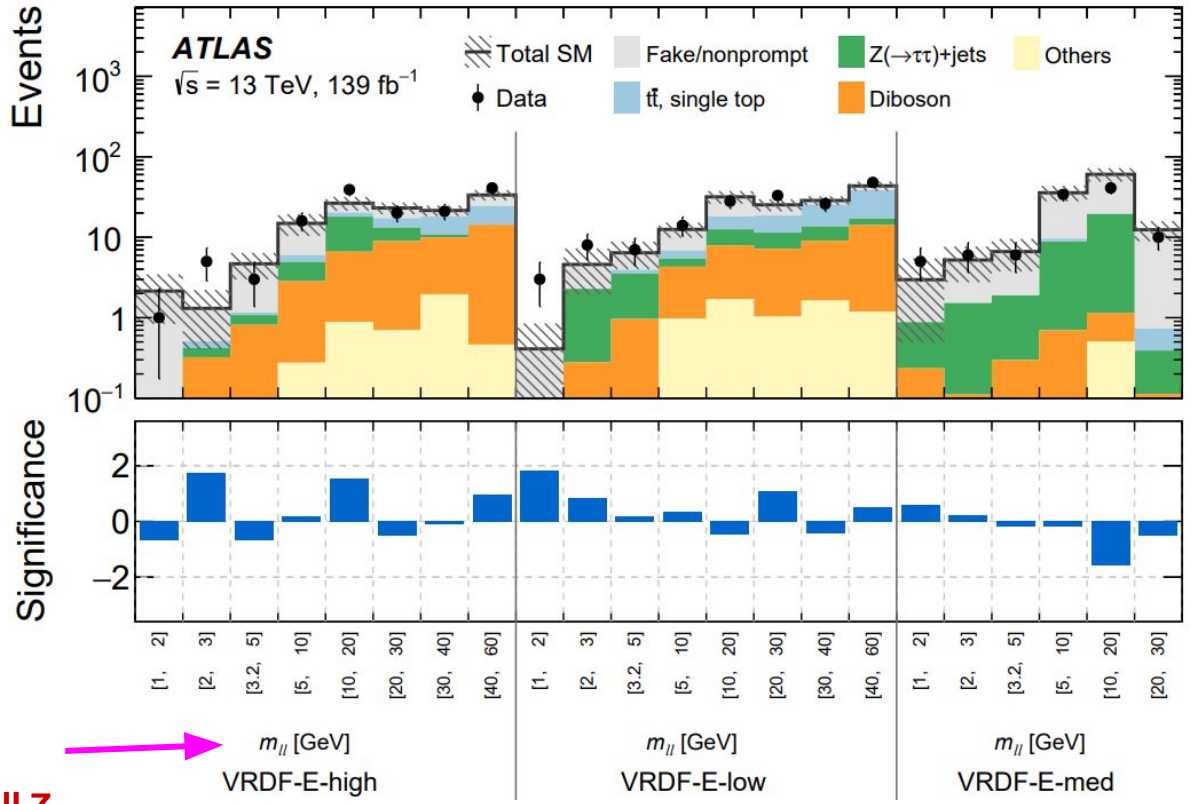

All binned in mll targeting off-shell Z

Electroweak Scenario

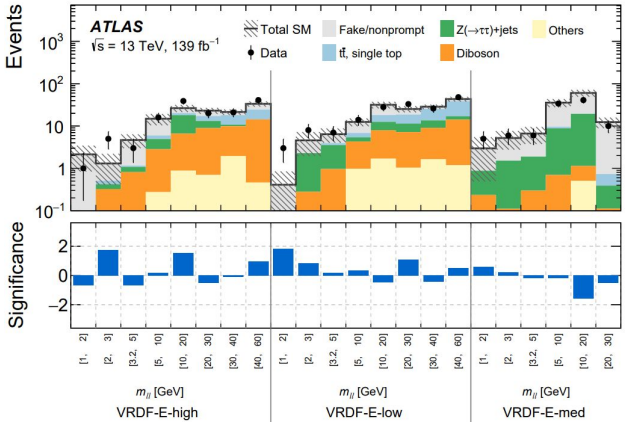

VBF Scenario

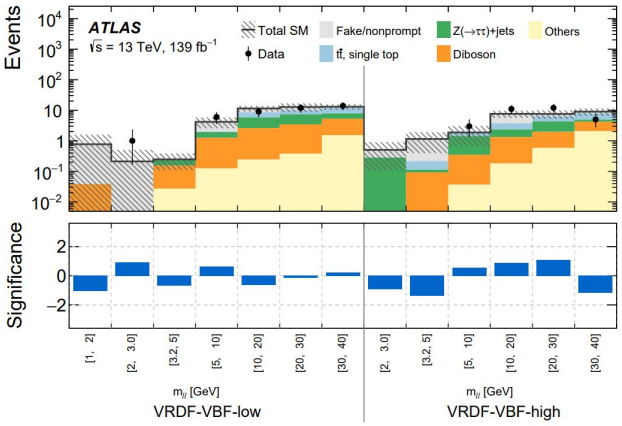

Slepton Scenario

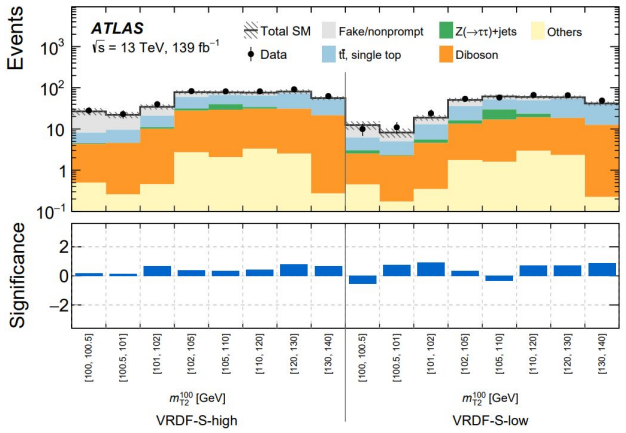

All yields are post fit, significances extracted via profiled likelihood approach. All are binned the same in CR/VR/SR

- VRDF-E-high, low, high MET
- Good agreement across all mll bins

- VRDF-VBF low and high pseudorapidty seperation
- Good agreement across all mll bins

- VRDF-S-high, low MET
- Good agreement across all MT2,100 bins

Electroweak Signal Regions

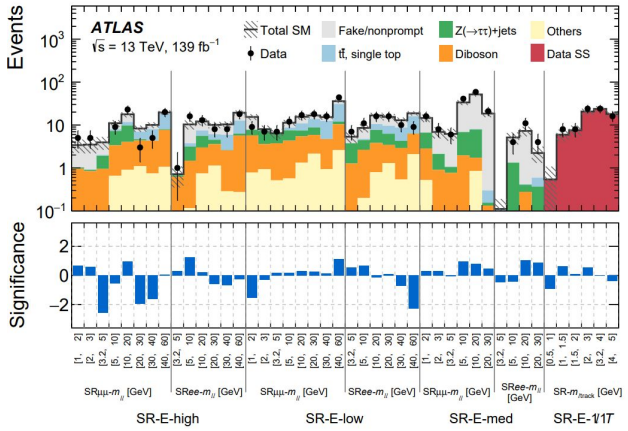

VBF Signal Regions

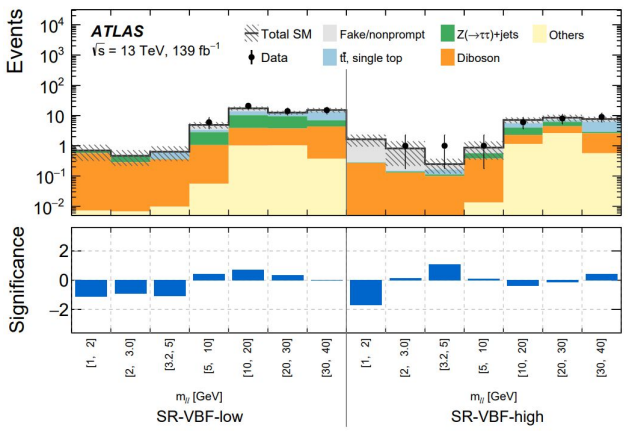

Slepton Signal Regions

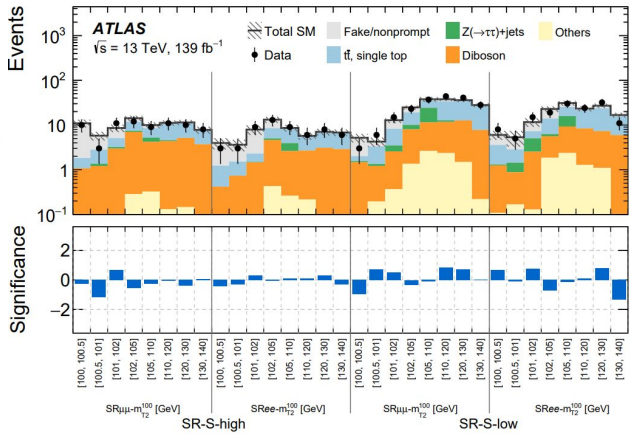

- Here we show the post fit yields for all signal regions detailed.
- We see the observed events agree within uncertainties with predicted background
- In particular we see nice agreement with the 1 lepton + 1 track signal regions which is entirely data-driven
- The VBF and slepton signal regions also see good agreement with the predicted background
- We extract model independent limits (see backup)
- We now show exclusion limits on compression scenarios under different mass parameter scenarios.

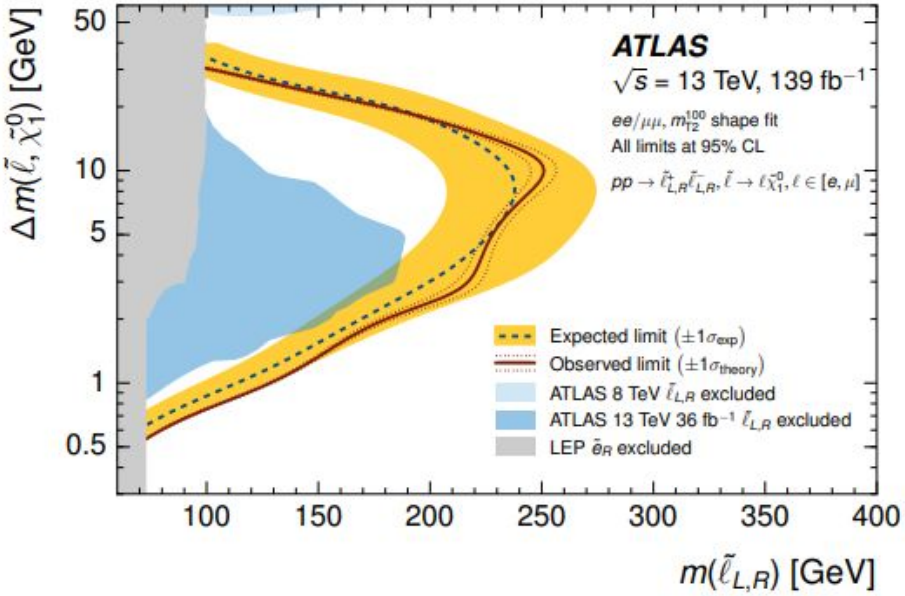

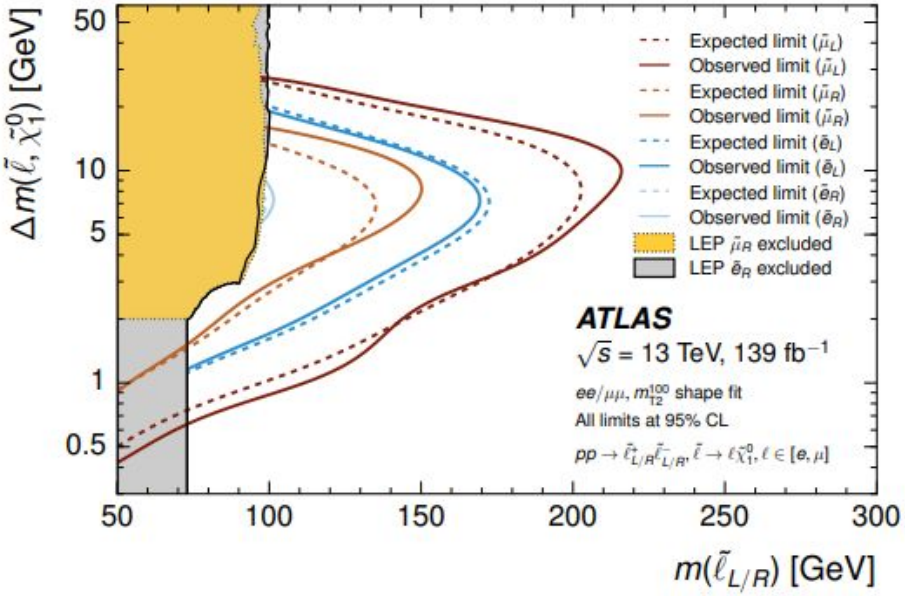

- The slepton analysis performs a shape fit in MT2 with a mass hypothesis of the LSP at 100 GeV
- Test two hypotheses
  - Degenerate sleptons (left)
  - Non-degenerate sleptons (right)
- Nice progress has been made to expand these exclusions from Run-I and early Run-II results.

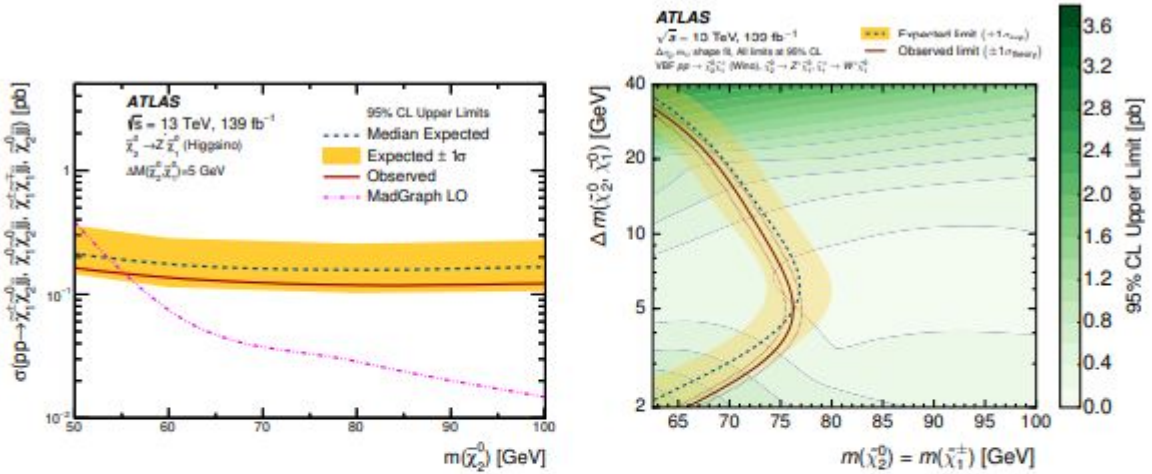

Figure 15: Expected 95% CL exclusion sensitivity (blue dashed line) and observed limits (red solid line) for simplified models of higgsino (left) and wino (right) production through VBF. A fit of signals to the $m_{\ell\ell}$ spectrum in the VBF signal regions is used to derive the limit. On the left, the limit for higgsinos is shown as a function of $m(\widetilde{\chi}_2^0)$ for a mass splitting of $\Delta m(\widetilde{\chi}_2^0, \widetilde{\chi}_1^0) = 5$ GeV (the chargino $\widetilde{\chi}_1^\pm$ mass is assumed to be halfway between the $\widetilde{\chi}_2^0$ and $\widetilde{\chi}_1^0$ masses). The yellow band indicates $\pm 1\sigma_{\text{exp}}$ from experimental systematic uncertainties and statistical uncertainties on the data yields. On the right the limit for winos is projected into the $\Delta m(\widetilde{\chi}_2^0, \widetilde{\chi}_1^0)$ vs. $m(\widetilde{\chi}_2^0)$ plane ($m(\widetilde{\chi}_2^0) = m(\widetilde{\chi}_1^\pm)$ is assumed for the wino/bino model). The red dotted line indicates the $\pm 1\sigma_{\text{theory}}$ from signal cross-section uncertainties and the colored map illustrates the 95% CL upper limits on the cross-section. The cross-section corresponds to the leading-order prediction from MG5_aMC@NLO for the process $pp \to \widetilde{\chi}_2^0 \widetilde{\chi}_1^\pm jj$ including the parton-level requirements described in Section 3. The contour lines represent steps of 0.2 pb.

TABLE X. *Left to right:* The first column indicates the inclusive signal region under study, defined as the union of the individual SRs defined in Sec. V and by upper bounds on $m_{\ell\ell}$ or m_{T2}^{100} in GeV. The $m_{\ell\ell}$ regions include events in both the 2ℓ and $1\ell 1T$ channels, while the m_{T2}^{100} regions only include 2ℓ events. The next two columns present observed (N_{obs}) and expected (N_{exp}) event yields in the inclusive signal regions. The latter are obtained by the background-only fit of the CRs, and the errors include both the statistical and systematic uncertainties. The next two columns show the observed 95% C.L. upper limits on the visible cross section ($\langle\epsilon\sigma\rangle_{\mathrm{obs}}^{95}$) and on the number of signal events (S_{obs}^{95}). The next column (S_{exp}^{95}) shows the 95% C.L. upper limit on the number of signal events, given the expected number (and $\pm 1\sigma$ deviations from the expectation) of background events. The last column indicates the discovery p-value [$p(s=0)$].

	Signal region	N_{obs}	N_{exp}	$\langle\epsilon\sigma\rangle_{\mathrm{obs}}^{95}$ [fb]	S_{obs}^{95}	S_{exp}^{95}	$p(s=0)$
SR-E	$m_{\ell\ell} < 1$	0	1.0 ± 1.0	0.022	3.0	$3.0^{+1.3}_{-0.0}$	0.50
	$m_{\ell\ell} < 2$	46	44 ± 6.8	0.15	21	19^{+7}_{-5}	0.38
	$m_{\ell\ell} < 3$	90	77 ± 12	0.29	41	31^{+11}_{-9}	0.18
	$m_{\ell\ell} < 5$	151	138 ± 18	0.38	52	43^{+16}_{-11}	0.24
	$m_{\ell\ell} < 10$	244	200 ± 19	0.62	86	49^{+26}_{-13}	0.034
	$m_{\ell\ell} < 20$	383	301 ± 23	0.95	132	61^{+22}_{-16}	0.0034
	$m_{\ell\ell} < 30$	453	366 ± 27	1.04	144	70^{+26}_{-20}	0.0065
	$m_{\ell\ell} < 40$	492	420 ± 30	0.96	134	74^{+29}_{-20}	0.027
	$m_{\ell\ell} < 60$	583	520 ± 35	0.97	135	84^{+32}_{-23}	0.063
SR-VBF	$m_{\ell\ell} < 2$	0	2.8 ± 1.6	0.022	3.0	$3.9^{+1.6}_{-0.9}$	0.50
	$m_{\ell\ell} < 3$	1	3.1 ± 1.7	0.030	3.6	$4.4^{+2.0}_{-1.0}$	0.50
	$m_{\ell\ell} < 5$	2	3.3 ± 1.7	0.035	4.8	$5.2^{+2.1}_{-1.1}$	0.50
	$m_{\ell\ell} < 10$	9	8.4 ± 2.7	0.068	9.5	$8.8^{+3.2}_{-2.2}$	0.43
	$m_{\ell\ell} < 20$	36	32 ± 5	0.14	20	16^{+6}_{-4}	0.27
	$m_{\ell\ell} < 30$	58	52 ± 7	0.19	26	21^{+8}_{-6}	0.28
	$m_{\ell\ell} < 40$	82	74 ± 10	0.24	33	27^{+10}_{-7}	0.27
SR-VBF-high	$m_{\ell\ell} < 2$	0	2.4 ± 1.1	0.022	3.0	$4.0^{+1.6}_{-0.9}$	0.50
	$m_{\ell\ell} < 3$	1	3.0 ± 1.4	0.025	3.5	$4.6^{+1.8}_{-1.2}$	0.50
	$m_{\ell\ell} < 5$	2	3.0 ± 1.4	0.034	4.7	$5.1^{+2.0}_{-1.3}$	0.50
	$m_{\ell\ell} < 10$	3	3.8 ± 1.7	0.041	5.6	$5.8^{+2.1}_{-1.3}$	0.50
	$m_{\ell\ell} < 20$	9	11.7 ± 2.8	0.055	8	$9^{+4}_{-2.3}$	0.50
	$m_{\ell\ell} < 30$	17	20 ± 5	0.079	11	$13^{+5}_{-3.2}$	0.50
	$m_{\ell\ell} < 40$	26	28 ± 6	0.10	14	15^{+6}_{-4}	0.50
SR-S	$m_{\mathrm{T2}}^{100} < 100.5$	24	27 ± 4.8	0.09	13	14^{+5}_{-4}	0.50
	$m_{\mathrm{T2}}^{100} < 101$	41	46 ± 6.5	0.11	16	18^{+7}_{-5}	0.50
	$m_{\mathrm{T2}}^{100} < 102$	91	82 ± 10	0.25	35	28^{+10}_{-8}	0.25
	$m_{\mathrm{T2}}^{100} < 105$	158	158 ± 17	0.30	41	41^{+16}_{-11}	0.50
	$m_{\mathrm{T2}}^{100} < 110$	243	242 ± 21	0.38	52	52^{+19}_{-14}	0.36
	$m_{\mathrm{T2}}^{100} < 120$	328	312 ± 24	0.51	71	60^{+22}_{-17}	0.26
	$m_{\mathrm{T2}}^{100} < 130$	419	388 ± 28	0.66	92	68^{+27}_{-18}	0.17
	$m_{\mathrm{T2}}^{100} < 140$	472	443 ± 31	0.69	95	74^{+28}_{-21}	0.19

Table 11: Observed event yields and fit results using a CR+SR background-only fit for the exclusive electroweakino signal regions. Background processes containing fewer than two prompt leptons are categorized as 'Fake/nonprompt'. The category 'Others' contains rare backgrounds from triboson, Higgs boson, and the remaining top-quark production processes listed in Table 1. Uncertainties in the fitted background estimates combine statistical and systematic uncertainties.

	SR bin [GeV]	[1,2]	[2,3]	[3.2,5]	[5,10]	[10,20]	[20,30]	[30,40]	[40,60]
SR-E-high ee	Observed			1	16	13	8	8	18
	Fitted SM events			0.7 ± 0.4	10.3 ± 2.5	12.1 ± 2.2	10.1 ± 1.7	10.4 ± 1.7	19.3 ± 2.5
	Fake/nonprompt			$0.03^{+0.19}_{-0.03}$	6.6 ± 2.7	4.6 ± 2.0	4.0 ± 1.5	4.4 ± 1.6	6.7 ± 2.3
	$t\bar{t}$, single top			$0.01^{+0.06}_{-0.01}$	0.59 ± 0.27	1.9 ± 0.5	1.6 ± 0.4	3.3 ± 0.6	6.4 ± 0.9
	Diboson			0.62 ± 0.23	1.4 ± 0.5	2.3 ± 0.7	2.5 ± 0.7	2.3 ± 0.6	5.4 ± 1.3
	$Z(\rightarrow \tau\tau)$+jets			$0.06^{+0.29}_{-0.06}$	1.7 ± 0.7	2.6 ± 1.2	0.93 ± 0.24	0.04 ± 0.04	0.62 ± 0.23
	Others			$0.000^{+0.004}_{-0.000}$	0.12 ± 0.05	0.74 ± 0.18	1.14 ± 0.19	0.29 ± 0.07	0.27 ± 0.14
SR-E-high $\mu\mu$	Observed	5	5	0	9	23	3	5	20
	Fitted SM events	3.4 ± 1.2	3.5 ± 1.3	3.9 ± 1.3	11.0 ± 2.0	17.8 ± 2.7	8.3 ± 1.4	10.1 ± 1.5	19.6 ± 2.3
	Fake/nonprompt	2.4 ± 1.2	2.6 ± 1.4	1.9 ± 1.0	3.1 ± 1.7	6.0 ± 2.8	1.3 ± 0.8	2.0 ± 0.9	1.4 ± 1.3
	$t\bar{t}$, single top	$0.01^{+0.06}_{-0.01}$	$0.01^{+0.06}_{-0.01}$	0.09 ± 0.07	0.67 ± 0.25	2.0 ± 0.5	2.4 ± 0.5	3.7 ± 0.9	10.2 ± 1.7
	Diboson	0.92 ± 0.32	0.84 ± 0.32	0.9 ± 0.4	2.7 ± 0.7	3.1 ± 0.8	3.3 ± 0.8	3.6 ± 0.8	6.6 ± 1.5
	$Z(\rightarrow \tau\tau)$+jets	$0.07^{+0.34}_{-0.07}$	$0.06^{+0.34}_{-0.06}$	1.0 ± 0.4	3.9 ± 0.9	5.7 ± 1.6	0.31 ± 0.25	$0.00^{+0.04}_{-0.00}$	0.31 ± 0.16
	Others	$0.032^{+0.035}_{-0.032}$	–	0.025 ± 0.018	0.66 ± 0.33	0.91 ± 0.14	1.10 ± 0.18	0.75 ± 0.16	1.06 ± 0.09
SR-E-med ee	Observed			0	4	11	4		
	Fitted SM events			0.11 ± 0.08	5.1 ± 1.6	7.3 ± 1.9	2.2 ± 0.9		
	Fake/nonprompt			$0.000^{+0.016}_{-0.000}$	3.8 ± 1.3	6.9 ± 2.0	1.6 ± 1.1		
	$t\bar{t}$, single top			$0.00^{+0.05}_{-0.00}$	$0.00^{+0.04}_{-0.00}$	$0.01^{+0.06}_{-0.01}$	$0.23^{+0.25}_{-0.23}$		
	Diboson			0.10 ± 0.05	0.10 ± 0.09	0.28 ± 0.26	$0.02^{+0.13}_{-0.02}$		
	$Z(\rightarrow \tau\tau)$+jets			$0.000^{+0.028}_{-0.000}$	1.2 ± 1.2	$0.1^{+0.5}_{-0.1}$	$0.3^{+0.6}_{-0.3}$		
	Others			$0.000^{+0.012}_{-0.000}$	–	–	–		
SR-E-med $\mu\mu$	Observed	16	8	6	41	59	21		
	Fitted SM events	14.6 ± 2.9	6.9 ± 2.1	6.2 ± 1.9	34 ± 4	52 ± 6	18.5 ± 3.2		
	Fake/nonprompt	7.9 ± 3.2	4.8 ± 2.1	5.1 ± 2.0	27 ± 5	44 ± 6	18.2 ± 3.2		
	$t\bar{t}$, single top	$0.01^{+0.06}_{-0.01}$	$0.01^{+0.06}_{-0.01}$	$0.00^{+0.05}_{-0.00}$	$0.12^{+0.13}_{-0.12}$	0.24 ± 0.08	$0.14^{+0.19}_{-0.14}$		
	Diboson	2.3 ± 0.8	0.9 ± 0.4	0.73 ± 0.24	1.9 ± 0.7	0.87 ± 0.26	0.13 ± 0.07		
	$Z(\rightarrow \tau\tau)$+jets	3.8 ± 1.8	1.2 ± 0.5	$0.3^{+0.6}_{-0.3}$	4.9 ± 1.6	6.1 ± 2.1	$0.02^{+0.29}_{-0.02}$		
	Others	0.5 ± 0.4	$0.000^{+0.026}_{-0.000}$	0.036 ± 0.015	0.019 ± 0.017	0.9 ± 0.6	–		
SR-E-low ee	Observed			7	11	16	16	10	9
	Fitted SM events			5.3 ± 1.5	8.6 ± 1.8	16.7 ± 2.5	15.5 ± 2.6	12.9 ± 2.1	18.8 ± 2.2
	Fake/nonprompt			1.6 ± 1.1	3.8 ± 1.8	6.2 ± 2.2	5.8 ± 2.3	4.2 ± 1.8	2.8 ± 1.4
	$t\bar{t}$, single top			0.015 ± 0.006	0.32 ± 0.30	2.8 ± 0.6	3.4 ± 1.1	4.5 ± 0.9	9.7 ± 1.5
	Diboson			1.3 ± 0.6	2.4 ± 0.8	3.0 ± 0.7	2.1 ± 0.7	2.4 ± 0.7	4.2 ± 1.0
	$Z(\rightarrow \tau\tau)$+jets			2.5 ± 1.1	1.8 ± 0.7	3.9 ± 1.3	2.8 ± 1.0	1.4 ± 0.7	$0.07^{+0.20}_{-0.07}$
	Others			$0.01^{+0.05}_{-0.01}$	0.20 ± 0.05	0.79 ± 0.23	1.3 ± 0.8	0.54 ± 0.09	2.10 ± 0.34
SR-E-low $\mu\mu$	Observed	9	7	7	12	17	18	16	44
	Fitted SM events	15.4 ± 2.4	8.0 ± 1.7	6.5 ± 1.6	11.3 ± 1.9	15.6 ± 2.3	16.7 ± 2.3	15.3 ± 2.0	35.9 ± 3.3
	Fake/nonprompt	7.7 ± 1.9	$0.3^{+0.6}_{-0.3}$	$0.01^{+0.22}_{-0.01}$	2.6 ± 1.3	4.7 ± 1.9	2.8 ± 1.6	2.8 ± 1.6	4.9 ± 2.3
	$t\bar{t}$, single top	$0.00^{+0.04}_{-0.00}$	0.26 ± 0.07	$0.01^{+0.06}_{-0.01}$	1.2 ± 0.5	3.4 ± 0.7	5.1 ± 1.5	7.8 ± 1.3	18.9 ± 2.7
	Diboson	4.9 ± 1.3	2.7 ± 0.7	3.2 ± 0.9	3.8 ± 0.9	4.1 ± 1.0	3.7 ± 0.9	3.8 ± 0.8	7.8 ± 1.6
	$Z(\rightarrow \tau\tau)$+jets	2.0 ± 0.7	3.8 ± 1.1	2.7 ± 1.2	3.2 ± 1.1	2.0 ± 1.2	2.9 ± 0.8	$0.01^{+0.27}_{-0.01}$	1.6 ± 0.6
	Others	0.8 ± 0.5	0.9 ± 0.8	0.52 ± 0.24	0.57 ± 0.16	1.32 ± 0.18	2.1 ± 0.4	0.94 ± 0.11	2.60 ± 0.20

Table 13: Observed event yields and fit results using a CR+SR background-only fit for the exclusive VBF signal regions. Background processes containing fewer than two prompt leptons are categorized as 'Fake/nonprompt'. The category 'Others' contains rare backgrounds from triboson, Higgs boson, and the remaining top-quark production processes listed in Table 1. Uncertainties in the fitted background estimates combine statistical and systematic uncertainties.

	SR bin [GeV]	[1,2]	[2,3]	[3.2,5]	[5,10]	[10,20]	[20,30]	[30,40]
SR–VBF–low	Observed	0	0	0	6	21	14	15
	Fitted SM events	0.7 ± 0.4	0.47 ± 0.25	0.64 ± 0.32	4.9 ± 1.2	17.3 ± 2.6	12.5 ± 1.8	15.2 ± 2.7
	$Z(\rightarrow \tau\tau)$+jets	$0.11^{+0.22}_{-0.11}$	0.17 ± 0.12	$0.009^{+0.018}_{-0.009}$	1.8 ± 0.7	6.4 ± 1.4	5.7 ± 1.3	2.6 ± 1.0
	Fake/nonprompt	$0.01^{+0.05}_{-0.01}$	$0.01^{+0.05}_{-0.01}$	$0.01^{+0.05}_{-0.01}$	1.5 ± 1.0	3.4 ± 2.0	$0.01^{+0.06}_{-0.01}$	$1.8^{+2.5}_{-1.8}$
	Diboson	0.57 ± 0.29	0.28 ± 0.17	0.35 ± 0.20	1.0 ± 0.4	2.8 ± 1.1	2.7 ± 1.004	4.0 ± 1.4
	$t\bar{t}$, single top	$0.01^{+0.04}_{-0.01}$	$0.01^{+0.05}_{-0.01}$	0.26 ± 0.18	0.55 ± 0.27	3.6 ± 1.3	3.1 ± 0.7	6.4 ± 1.1
	Others	0.007 ± 0.007	0.007 ± 0.004	$0.01^{+0.05}_{-0.01}$	0.056 ± 0.026	1.0 ± 0.4	1.03 ± 0.32	0.37 ± 0.13
SR–VBF–high	Observed	0	1	1	1	6	8	9
	Fitted SM events	1.6 ± 0.7	0.8 ± 0.6	0.25 ± 0.13	0.9 ± 0.5	7.1 ± 1.5	8.5 ± 2.2	7.7 ± 1.5
	$Z(\rightarrow \tau\tau)$+jets	$0.009^{+0.018}_{-0.009}$	$0.010^{+0.021}_{-0.010}$	$0.012^{+0.026}_{-0.012}$	$0.19^{+0.29}_{-0.19}$	1.7 ± 0.8	1.8 ± 1.3	0.27 ± 0.09
	Fake/nonprompt	1.4 ± 0.7	0.7 ± 0.6	$0.08^{+0.11}_{-0.08}$	$0.3^{+0.5}_{-0.3}$	1.5 ± 1.0	$1.4^{+1.5}_{-1.4}$	1.2 ± 1.2
	Diboson	0.27 ± 0.17	0.13 ± 0.11	0.10 ± 0.05	0.37 ± 0.19	1.1 ± 0.5	1.8 ± 0.7	2.0 ± 0.8
	$t\bar{t}$, single top	$0.01^{+0.05}_{-0.01}$	$0.01^{+0.06}_{-0.01}$	$0.05^{+0.09}_{-0.05}$	$0.01^{+0.06}_{-0.01}$	1.7 ± 0.6	0.9 ± 0.6	3.5 ± 0.8
	Others	– –	– –	– –	$0.01^{+0.02}_{-0.01}$	1.2 ± 0.4	2.6 ± 1.5	0.57 ± 0.21

Table 14: Observed event yields and fit results using a CR+SR background-only fit for the exclusive slepton signal regions. Background processes containing fewer than two prompt leptons are categorized as 'Fake/nonprompt'. The category 'Others' contains rare backgrounds from triboson, Higgs boson, and the remaining top-quark production processes listed in Table 1. Uncertainties in the fitted background estimates combine statistical and systematic uncertainties.

	SR bin [GeV]	[100,100.5]	[100.5,101]	[101,102]	[102,105]	[105,110]	[110,120]	[120,130]	[130,140]
SR-S-high ee	Observed	3	3	9	13	9	6	8	6
	Fitted SM events	4.0 ± 1.1	3.6 ± 1.0	7.9 ± 1.9	13.2 ± 2.1	8.6 ± 1.4	5.7 ± 1.0	7.0 ± 1.2	6.8 ± 1.1
	Fake/nonprompt	2.7 ± 1.1	2.1 ± 1.0	5.6 ± 1.9	4.7 ± 1.9	$0.2^{+0.5}_{-0.2}$	$0.01^{+0.17}_{-0.01}$	$0.01^{+0.17}_{-0.01}$	$0.00^{+0.15}_{-0.00}$
	$t\bar{t}$, single top	0.8 ± 0.4	0.8 ± 0.5	0.8 ± 0.4	3.5 ± 0.7	4.5 ± 1.2	3.0 ± 0.7	3.9 ± 0.9	3.9 ± 0.9
	Diboson	0.42 ± 0.16	0.68 ± 0.23	1.4 ± 0.4	4.2 ± 1.1	2.4 ± 0.7	2.5 ± 0.7	3.0 ± 0.8	2.8 ± 0.7
	$Z(\rightarrow \tau\tau)$+jets	$0.00^{+0.08}_{-0.00}$	$0.00^{+0.18}_{-0.00}$	0.027 ± 0.012	0.38 ± 0.16	1.32 ± 0.31	$0.00^{+0.12}_{-0.00}$	$0.02^{+0.22}_{-0.02}$	$0.00^{+0.19}_{-0.00}$
	Others	0.0 ± 0.0	$0.06^{+0.11}_{-0.06}$	0.09 ± 0.05	0.43 ± 0.32	0.26 ± 0.14	$0.2^{+0.5}_{-0.2}$	$0.06^{+0.08}_{-0.06}$	0.05 ± 0.05
SR-S-high $\mu\mu$	Observed	10	3	11	12	9	11	10	8
	Fitted SM events	11.0 ± 2.2	5.8 ± 1.3	8.6 ± 1.6	14.2 ± 1.9	10.0 ± 1.5	11.2 ± 1.6	11.5 ± 1.5	7.8 ± 1.4
	Fake/nonprompt	9.1 ± 2.2	3.0 ± 1.1	3.5 ± 1.4	2.4 ± 1.2	1.5 ± 1.0	$0.7^{+0.8}_{-0.7}$	$0.4^{+0.5}_{-0.4}$	$0.19^{+0.33}_{-0.19}$
	$t\bar{t}$, single top	0.8 ± 0.5	1.5 ± 0.5	1.9 ± 0.5	4.4 ± 0.8	3.3 ± 0.7	5.9 ± 1.1	5.9 ± 0.9	3.9 ± 1.3
	Diboson	1.1 ± 0.4	1.2 ± 0.4	2.9 ± 1.3	6.7 ± 1.7	3.9 ± 1.1	4.2 ± 1.0	5.0 ± 1.3	3.7 ± 0.9
	$Z(\rightarrow \tau\tau)$+jets	$0.00^{+0.19}_{-0.00}$	0.15 ± 0.04	0.22 ± 0.19	0.40 ± 0.34	1.03 ± 0.34	0.19 ± 0.12	$0.00^{+0.19}_{-0.00}$	$0.00^{+0.21}_{-0.00}$
	Others	$0.000^{+0.019}_{-0.000}$	0.029 ± 0.017	0.09 ± 0.05	0.29 ± 0.14	0.32 ± 0.22	0.13 ± 0.11	0.15 ± 0.12	0.06 ± 0.05
SR-S-low ee	Observed	8	5	15	19	30	24	32	11
	Fitted SM events	6.0 ± 1.4	5.3 ± 2.1	11.6 ± 2.5	22.9 ± 3.3	31 ± 4	23.3 ± 3.0	27.1 ± 3.1	16.8 ± 2.1
	Fake/nonprompt	2.4 ± 1.2	2.5 ± 1.2	4.4 ± 2.0	9.0 ± 2.8	5.7 ± 2.7	$1.6^{+1.7}_{-1.6}$	3.4 ± 2.3	1.0 ± 0.9
	$t\bar{t}$, single top	2.3 ± 0.9	1.4 ± 0.5	2.2 ± 0.7	7.6 ± 1.7	9.6 ± 1.7	13.3 ± 3.3	16.4 ± 3.0	9.8 ± 1.5
	Diboson	1.1 ± 0.6	0.71 ± 0.30	2.4 ± 0.8	3.8 ± 1.3	6.9 ± 2.1	7.1 ± 2.1	6.2 ± 2.0	5.9 ± 1.6
	$Z(\rightarrow \tau\tau)$+jets	$0.1^{+0.4}_{-0.1}$	$0.6^{+2.0}_{-0.6}$	2.5 ± 2.4	$0.7^{+1.5}_{-0.7}$	6.5 ± 2.2	$0.01^{+0.26}_{-0.01}$	$0.03^{+0.30}_{-0.03}$	$0.000^{+0.032}_{-0.000}$
	Others	0.11 ± 0.06	0.17 ± 0.15	0.13 ± 0.09	1.8 ± 0.9	2.4 ± 2.4	1.3 ± 1.2	1.1 ± 1.0	0.042 ± 0.034
SR-S-low $\mu\mu$	Observed	3	6	15	23	37	44	41	28
	Fitted SM events	5.2 ± 1.1	4.3 ± 1.0	12.8 ± 1.8	24.8 ± 2.6	38 ± 5	37.8 ± 3.3	36.0 ± 3.4	28.0 ± 2.7
	Fake/nonprompt	3.2 ± 1.0	0.9 ± 0.7	4.6 ± 1.5	5.6 ± 1.8	2.8 ± 1.7	3.8 ± 2.0	1.5 ± 1.2	$0.00^{+0.10}_{-0.00}$
	$t\bar{t}$, single top	0.45 ± 0.18	2.0 ± 0.5	4.7 ± 1.0	9.1 ± 1.6	10.6 ± 1.9	21.2 ± 2.9	21.8 ± 2.6	20.2 ± 2.7
	Diboson	1.4 ± 0.5	1.02 ± 0.34	2.2 ± 0.8	6.7 ± 1.9	8.8 ± 2.6	9.4 ± 2.6	11.2 ± 3.2	7.5 ± 2.2
	$Z(\rightarrow \tau\tau)$+jets	$0.09^{+0.16}_{-0.09}$	$0.1^{+0.5}_{-0.1}$	0.9 ± 0.4	2.1 ± 1.0	13 ± 5	1.0 ± 0.6	$0.02^{+0.29}_{-0.02}$	$0.00^{+0.26}_{-0.00}$
	Others	0.032 ± 0.026	0.19 ± 0.11	0.37 ± 0.19	1.4 ± 0.8	2.6 ± 1.5	2.4 ± 1.2	1.5 ± 0.8	0.22 ± 0.13